Comparative Biochemistry and Physiology, Part C 290 (2025) 110129

Contents lists available at ScienceDirect

Comparative Biochemistry and Physiology, Part C

journal homepage: www.elsevier.com/locate/cbpc

Venom variation and ontogenetic changes in the *Crotalus molossus* complex: Insights into composition, activities, and antivenom neutralization

Miguel Borja [a], Gamaliel Castañeda-Gaytán [a], Alejandro Alagón [b], Jason L. Strickland [c], Christopher L. Parkinson [d], Areli Gutiérrez-Martínez [a], Bruno Rodriguez-López [a], Vanessa Zarzosa [b], Bruno Lomonte [e], Anthony J. Saviola [f], Julián Fernández [e], Cara F. Smith [f], Kirk C. Hansen [f], Armando Pérez-Robles [b], Sebastián Castañeda-Pérez [g], Samuel R. Hirst [h], Felipe Olvera-Rodríguez [b], Leonardo Fernández-Badillo [i], Jesús Sigala [j], Jason Jones [k], Carlos Montaño-Ruvalcaba [k], Ricardo Ramírez-Chaparro [k], Mark J. Margres [h], Gerardo Acosta-Campaña [l], Edgar Neri-Castro [a,*]

[a] *Facultad de Ciencias Biológicas, Universidad Juárez del Estado de Durango, Av. Universidad s/n. Fracc. Filadelfia, C.P. 35010 Gómez Palacio, Dgo., Mexico*
[b] *Instituto de Biotecnología, Universidad Nacional Autónoma de México, Avenida Universidad 2001, Chamilpa, C.P. 62210 Cuernavaca, Mor., Mexico*
[c] *Department of Biology, University of South Alabama, 5871 USA Dr. N., Mobile, AL 36688, USA*
[d] *Department of Biological Sciences, Clemson University, Clemson, SC 29634, USA*
[e] *Instituto Clodomiro Picado, Facultad de Microbiología, Universidad de Costa Rica, San José 11501, Costa Rica*
[f] *Department of Biochemistry and Molecular Genetics, University of Colorado Denver, Aurora, CO, USA*
[g] *Facultad de Ciencias Químicas, Universidad Juárez del Estado de Durango, Av. Artículo 123 s/n. Fracc. Filadelfia, Apartado Postal No. 51, C.P. 35010 Gómez Palacio, Dgo., Mexico*
[h] *Department of Integrative Biology, University of South Florida, Tampa, FL 33620, USA.*
[i] *Laboratorio de Interacciones Biológicas, Centro de Investigaciones Biológicas, Universidad Autónoma del Estado de Hidalgo, km 4.5 carretera Pachuca-Tulancingo, Col. Carboneras, C.P. 42184 Mineral de la Reforma, Hidalgo, Mexico.*
[j] *Universidad Autónoma de Aguascalientes, Centro de Ciencias Básicas, Departamento de Biología, Colección Zoológica, Aguascalientes, Mexico*
[k] *Herp.mx A.C., Villa de Álvarez, Colima, Mexico.*
[l] *Museo Itinerante de Vida Animal. Cavani 32-C. Mallorca, Hermosillo, Sonora, Mexico*

ARTICLE INFO

Edited by Martin Grosell

Keywords:
Crotoxin
Crotamine
Myotoxin
Mexico
LD_{50}
Antivenom

ABSTRACT

The *Crotalus molossus* complex consists of five to seven phylogenetically related lineages of black-tailed rattlesnakes widely distributed in Mexico. While previous studies have noted venom variation within specific lineages of the *Crotalus molossus* complex, a comprehensive characterization of interspecific and ontogenetic venom variations, their functional implications, and the neutralizing ability of the Mexican antivenom against these variants remains largely unexamined. Herein, using two proteomic approaches for five lineages (*C. basiliscus*, *C. m. molossus*, *C. m. nigrescens*, *C. m. oaxacus*, and *C. ornatus*) of the *C. molossus* complex we characterized the number of toxins and their relative abundance in the venom of individuals of varying sizes. All five lineages undergo ontogenetic venom composition shifts associated with snake length. However, the pattern of ontogenetic shifts varied among lineages. In some lineages, these shifts led to significant differences in proteolytic, phospholipase A_2, and fibrinogenolytic activities. Venom in smaller *C. basiliscus*, *C. m. nigrescens*, and *C. m. oaxacus* individuals had lower LD_{50} values (more lethal) in mice. Whereas the venom lethality of *C. m. nigrescens* (both juvenile and adult) and *C. m. oaxacus* (adult) was several times higher in a mammalian (mouse) model than in a reptilian (iguana) model. Antivipmyn® showed different neutralizing potencies toward venom pools. Overall, our results indicated that even among closely related rattlesnake lineages, venom phenotypes may vary greatly, impacting their function and the efficacy of antivenom neutralization.

* Corresponding author.
E-mail address: edgare.neri@secihti.mx (E. Neri-Castro).

https://doi.org/10.1016/j.cbpc.2025.110129
Received 12 November 2024; Received in revised form 15 December 2024; Accepted 20 January 2025
Available online 30 January 2025

1. Introduction

Snake venom is a functional trait and a key adaptative innovation that evolved to aid prey capture. Snake venoms often vary in composition at inter- and intraspecific levels (Casewell et al., 2020), and evidence suggests that both abiotic factors (e.g., temperature differences) and biotic factors (e.g., prey diversity, availability, and resistance) may directly or indirectly contribute to this variation to a certain degree (Gren et al., 2017; Margres et al., 2021b; Smith et al., 2023; Sousa et al., 2021; Strickland et al., 2018b; Zancolli et al., 2019). Additionally, large-bodied snake species that undergo drastic changes in size from birth to adulthood frequently exhibit ontogenetic changes in venom composition, as the venom phenotype adaptively changes throughout its life history according to changes in its trophic and defensive actions (Andrade and Abe, 1999; Cipriani et al., 2017; Hogan et al., 2024; Mackessy et al., 2006).

Rattlesnakes (genera *Crotalus* and *Sistrurus*) belong to the family Viperidae and are distributed only in the Americas, with Mexico containing the largest number of species (Myers et al., 2024; Uetz et al., 2024). Rattlesnake venoms are composed mostly of proteins grouped into toxin families which differ in presence and abundance across species and within species (geographically and ontogenetically). Despite the high diversity of rattlesnakes in Mexico, the venom composition of only some species distributed throughout the country has been characterized. Among the different toxin families identified in rattlesnake venoms, phospholipases A_2 (PLA_2), snake venom metalloproteinases (SVMPs), and snake venom serine proteases (SVSPs) are the most common and abundant (Arnaud et al., 2021; Arnaud-Franco et al., 2018; Borja et al., 2023, 2018a, 2018b, 2013; Castro et al., 2013; Colis-Torres et al., 2022; Durban et al., 2017; Franco-Servín et al., 2021; Grabowsky et al., 2023; Mackessy et al., 2018; Martínez-Romero et al., 2013; Neri-Castro et al., 2022, 2020; Pozas-Ocampo et al., 2020; Saviola et al., 2017; Zarzosa et al., 2023). These three families also cause the most severe pathophysiological effects following envenomation (Oliveira et al., 2022). Small basic non-enzymatic myotoxins (MYO), also referred to as crotamine or myotoxin *a*, are often abundant in the venom of some rattlesnake species (Hirst et al., 2024; Durban et al., 2017; Smith et al., 2023; Strickland et al., 2018a) while completely absent in the venom of others (Grabowsky et al., 2023; Grabowsky and Mackessy, 2019; Mackessy et al., 2018; Saviola et al., 2017). Additionally, the abundance of MYO in the venom of snakes of the same species may vary ontogenetically and geographically (Hirst et al., 2024; Margres et al., 2017, 2015; Saviola et al., 2015; Smith et al., 2023; Tasima et al., 2020), although the ecological significance of this variation remains unclear.

Venom variation may also have medical implications, as different toxin compositions can lead to dissimilar clinical symptoms and severity in envenomated patients (Bosak et al., 2014; Keyler et al., 2020; Massey et al., 2012; Vohra et al., 2008). Additionally, both interspecific and ontogenetic venom variations represent challenges to antivenom efficacy. For instance, distinct neutralizing potencies against the venom of viperids distributed in Mexico have been reported for the two antivenoms available in this country: Antivipmyn®(SILANES) and Laboratorios de Biologicos y Reactivos de Mexico S. A. de C. V. (BIRMEX) (Guadarrama-Martínez et al., 2024; Sánchez et al., 2020). Thus, testing the antivenom efficacy to recognize and neutralize venoms of different species and age classes is key to the continuous improvement of antivenoms.

The *Crotalus molossus* complex is a phylogenetically related group of black-tailed rattlesnakes (Anderson and Greenbaum, 2012; Myers et al., 2024; Muñoz-Mora et al., 2022; Wüster et al., 2005), currently comprising four species (*C. basiliscus*, C. *estabanesis*, *C. ornatus*, and *C. totonacus*) and three subspecies (*C. m. molossus*, *C. m. nigrescens*, and *C. m. oaxacus*). However, it has been suggested that the current subspecies within the *C. molossus* complex may be elevated to species status under a phylogenetic concept (Muñoz-Mora et al., 2022). *C. basiliscus* and *C. totonacus* are the largest lineages with a total body length maximum (TBL_{max}) of 170 cm in males and 204 cm in females for *C. basiliscus*, and 160 cm in males and 166 cm in females for *C. totonacus*. TBL_{max} of the remaining five lineages likely do not exceed 150 cm (Ernst and Ernst, 2011; Anderson and Greenbaum, 2012). The TBL of newborn individuals in all lineages is usually no <20 cm (Ernst and Ernst, 2011). *Crotalus basiliscus*, *C. estabanensis*, *C. m. nigrescens*, *C. totonacus* and *C. m. oaxacus* are distributed exclusively throughout Mexico, whereas *C. m. molossus* and *C. ornatus* are found in parts of northern Mexico and the southern United States (Fig. 1) (Anderson and Greenbaum, 2012; Ernst and Ernst, 2011). Currently, boundaries among lineages in the *C. molossus* complex are not entirely clear, and intergradation among species and subspecies is likely (Anderson and Greenbaum, 2012; Muñoz-Mora et al., 2022; Myers et al., 2024). Due to their wide distribution, populations of the same lineage and among lineages in the *C. molossus* complex may be found in a variety of habitats, including upland pine-oak, cloud forest, mesquite-grassland, chaparral, desert, tropical forest, with altitudes ranging from near sea level to 3150 m.a.s.l. (Ernst and Ernst, 2011). Thus, it is plausible that individuals across and within lineages in the *C. molossus* complex face different ecological pressures, which may be reflected in differences in the venom composition.

In Mexico, approximately 4000 cases of snakebite envenomation are reported each year, with an average mortality of 34 deaths per year (Neri-Castro et al., 2021). However, this information may be underestimated due to underreporting and incomplete clinical data. Although the species involved in these incidents are not recorded in Mexico, it is important to note that, based on our experience and communication with medical professionals, lineages within the *C. molossus* complex should be considered of medical significance due to the frequent reports of envenomations. Additionally, these lineages are known for their restless and defensive temperament, and they are relatively common in the northern part of the country, which increases the risk of encounters.

Currently, only the venom proteomes of *C. basiliscus* (Segura et al., 2017) and *C. m. molossus* (Jimenez-Canale et al., 2024) have been reported; however, in both cases, only pooled venoms were analyzed, thus limiting the identification of individual variation. Studies using reverse-phase high-performance liquid chromatography (RP-HPLC), sodium dodecyl sulfate-polyacrylamide gel electrophoresis (SDS-PAGE), and mass spectrometry of a few toxins have reported geographic and ontogenetic differences in the abundance of MYO, SVSP, PLA_2, and SVMP in venoms of *C. basiliscus* and *C. m. nigrescens*, resulting in differences in biological and enzymatic activities. Additionally, Mexican antivenoms showed poor recognition and neutralization of low molecular mass toxins such as MYO (Borja et al., 2023, 2018b; Colis-Torres et al., 2022). For the lineages such as *C. ornatus* and *C. totonacus*, only the isolation and characterization of a few toxins have been described (Meléndez-Martínez et al., 2020; Rael et al., 1997; Rivas Mercado et al., 2020). Additionally, no information is available on the venom composition of *C. estabanensis* and *C. m. oaxacus*.

Herein, we used bottom-up proteomics to comprehensively characterize the venom composition of *C. basiliscus*, *C. m. molossus*, *C. m. nigrescens*, *C. m. oaxacus*, and *C. ornatus* from Mexico, both individually and as pooled samples. We described the patterns of ontogenetic venom shifts and their effects on the biological activity of each lineage. Additionally, we assessed the efficacy of the Mexican antivenom Antivipmyn® in recognizing and neutralizing the venom from these medically important rattlesnake lineages.

2. Materials and methods

2.1. Ethical and regulatory approvals

The use of animals was granted by the bioethics committee of the Institute of Biotechnology at UNAM, project #379. Collection of venom samples was conducted under permits (DGVS/10362/21; DGVS/04236/22) issued by the Secretariat of Environment and Natural Resources of

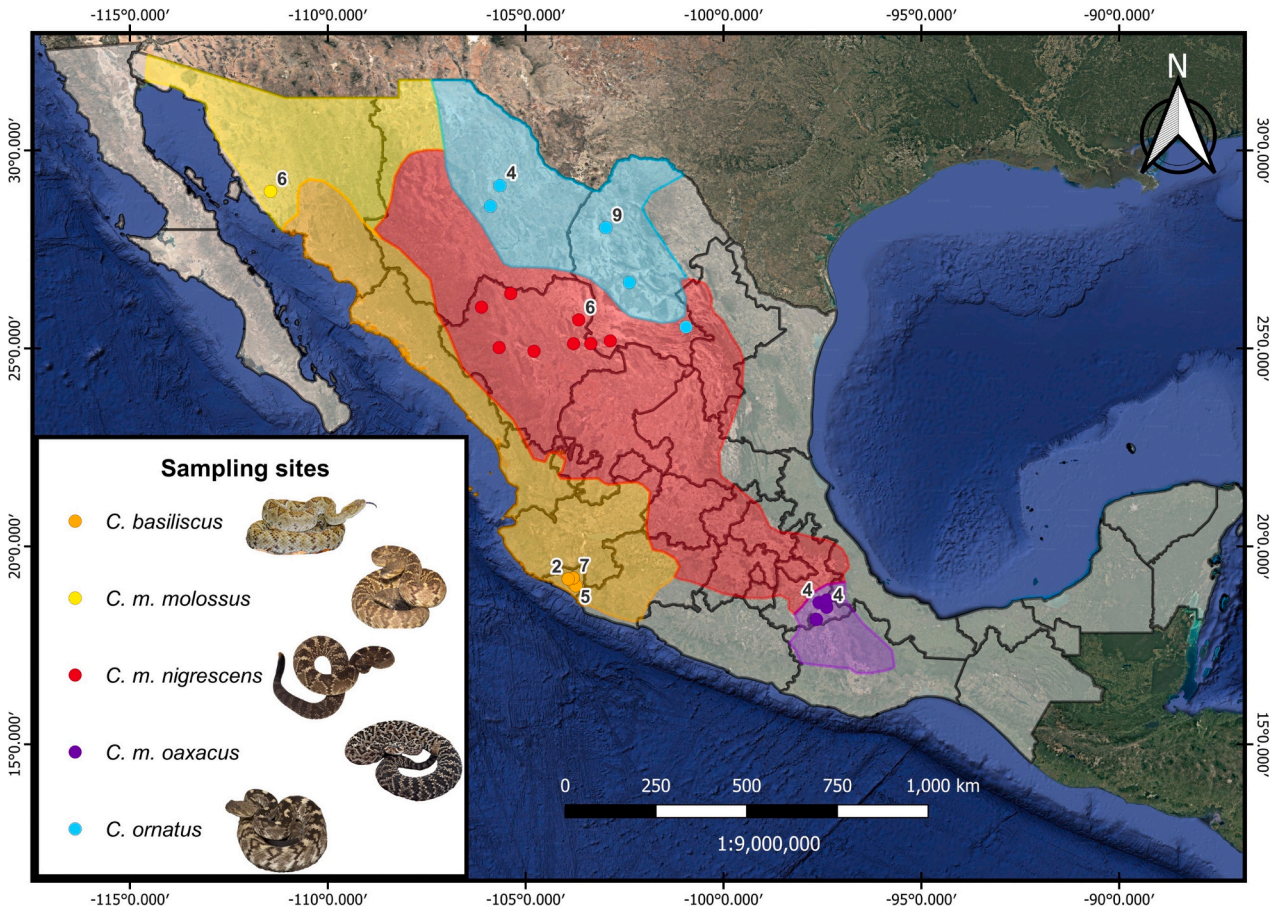

Fig. 1. Map depicting the geographic distribution of *Crotalus basiliscus*, *C. molossus molossus*, *C. m. nigrescens*, *C. m. oaxacus*, and *C. ornatus* in Mexico. Dots indicate the geographic origins of the specimens used in this study. The numbers represent the count of individuals collected at each dot. Dots without numbers indicate that only a single individual was collected.

the Mexican government (SEMARNAT). We worked with iguanas (*Ctenosaura pectinata*), which were acquired from the "Unidad de Manejo Ambiental Criadero de Iguana Barranca Honda", registration SEMARNAT-UMA-INT-028-MOR.

2.2. Experimental animals used in this research

Venom was obtained from individuals of *C. basiliscus* ($n = 14$), *C. m. molossus* ($n = 6$), *C. m. nigrescens* ($n = 13$), *C. m. oaxacus* ($n = 10$), and *C. ornatus* ($n = 16$) were collected from different localities in Mexico (Fig. 1, Table 1). We attempted to reduce the influence of geographic variation on venom variability by collecting individuals close to one another (e.g. <100 km distance; see Fig. 1). Snout–vent length (SVL), total body length (TBL), and sex were recorded for most individuals. We sampled individuals of differing SVLs to increase the chance of detecting ontogenetic differences in the venom composition (Table 1). For *C. ornatus*, we could not cover a complete spectrum of SVL in one locality thus, aiming to have a broader range of sizes, individuals from two different states from Mexico (Coahuila and Chihuahua) were analyzed.

For experiments involving median lethal doses (LD_{50}) and antivenom neutralization, ICR strain mice of either sex, weighing between 18 and 20 g, were employed. The mice were given access to food ad libitum and were kept on a controlled light-dark cycle. Additionally, we used the black iguana (*Ctenosaura pectinata*) as a reptilian model to evaluate the lethality of venoms. Black iguanas aged between 4 and 8 months were purchased from the UMA Barranca Honda. Specimens were housed in plastic containers in groups of three and maintained at a temperature of 28 °C, with food and water ad libitum.

2.3. Snake venoms and antivenom

Venoms were extracted manually by inducing the snakes to bite a parafilm-covered sterile plastic cup and centrifuged at 13,000 rpm to remove sedimented debris. Then, venoms were lyophilized in a FreeZone 2.5 Liter Benchtop Freeze Dryer (Labconco) and stored at −20 °C until use. We generated two representative venom pools of smaller and larger individuals of each lineage (Table 3). Each venom pool only included venoms with similar electrophoretic profile (see below). Ten milligrams of individual or pooled venoms were redissolved in phosphate-buffered saline (PBS, pH 7.2) and the protein concentration was determined using Pierce® Bicinchoninic Acid (BCA) Protein Assay (Thermo Scientific), using bovine serum albumin (BSA) as a standard, according to the manufacturer's protocols.

The antivenom Antivipmyn® (batch number: B-0D-32, with an expiration date of March 2024) was used for immunorecognition and neutralization tests, with a protein concentration of 6.14 mg/mL. This antivenom is produced using the venom of *Bothrops asper* and *Crotalus simus* as immunogens. It is important to note that although *C. simus* is phylogenetically close to the *C. molossus* complex, its venom is rich in crotoxin (CTX) homologs (Castro et al., 2013; Durban et al., 2017), a component previously detected in only one lineage (*C. basiliscus*) of the *C. molossus* complex. According to its specifications, a vial of Antivipmyn® neutralizes the lethality of no less than 780 LD_{50} of *B. asper* and no less than 790 LD_{50} of *Crotalus* sp. venoms.

Table 1
Metadata for specimens across the five lineages in the *C. molossus* complex.

Venom	Locality	Sex	SVL (cm)	Venom	Locality	Sex	SVL (cm)
CBA15	Coquimatlan, Colima	M	39	CMO10	Cacaloapan, Puebla	ND	36.9
CBA14	Coquimatlan, Colima	ND	45.8	CMO08	Tehuacan, Puebla	F	38
CBA05	Ixtlahuacan, Colima	ND	46.5	CMO02	Cacaloapan, Puebla	F	40
CBA06	Ixtlahuacan, Colima	ND	49	CMO130	San Jose Trujapan, Oaxaca	M	53
CBA08	Coquimatlan, Colima	ND	49.7	CMO11	Tehuacan, Puebla	F	56.5
CBA04	Ixtlahuacan, Colima	ND	51	CMO09	Cacaloapan, Puebla	ND	67.6
CBA09	Coquimatlan, Colima	F	52.5	CMO06	Azumbilla, Puebla	M	75.5
CBA12	Coquimatlan, Colima	M	133	CMO07	Tehuacan, Puebla	M	81.5
CBA11	Coquimatlan, Colima	M	136	CMO03	Cacaloapan, Puebla	M	89
CBA10	Coquimatlan, Colima	M	139	CMO05	Tehuacan, Puebla	M	99
CBA07	Ixtlahuacan, Colima	F	141	CO16	Aldama, Chihuahua	M	45.5
CBA16	Coquimatlan, Colima	ND	145	CO10	Aldama, Chihuahua	M	51.5
CBA13	Coquimatlan, Colima	M	150	CO15	Aldama, Chihuahua	M	59.5
CBA03	La Salada, Colima	F	157	CO09	Ramos Arizpe, Coahuila	M	67.5
CMM08	Hermosillo, Sonora	M	49.5	CO08	Ocampo, Coahuila	F	73
CMM09	Hermosillo, Sonora	F	57.6	CO07	Ocampo, Coahuila	F	74.5
CMM07	Hermosillo, Sonora	M	63.5	CO04	Ocampo, Coahuila	F	77
CMM05	Hermosillo, Sonora	F	64.5	CO13	Ocampo, Coahuila	F	78
CMM04	Hermosillo, Sonora	M	70.3	CO19	Ocampo, Coahuila	F	79
CMM06	Hermosillo, Sonora	M	75	CO14	Ocampo, Coahuila	M	81
CMN49	Guanacevi, Durango	ND	28	CO18	Ocampo, Coahuila	M	83
CMN50	Santiago Papasquiaro, Durango	ND	28.7	CO12	Ocampo, Coahuila	M	84
CMN44	Its mother is CMN41	ND	29	CO06	Ocampo, Coahuila	M	86
CMN43	Its mother is CMN41	ND	30.5	CO05	Santa Eulalia, Chihuahua	M	87
CMN40	Dinamita, Durango	F	59.5	CO03	Ocampo, Coahuila	M	90.5
CMN39	Torreón, Coahuila	F	62	CO11	Aldama, Chihuahua	F	95
CMN41	Dinamita, Durango	F	64				
CMN31	Puerto de Coneto, Durango	F	65.5				
CMN51	Pedriceña, Durango	M	78.5				
CMN06	Agua Puerca, Durango	F	80				
CMN52	Dinamita, Durango	M	80				
CMN46	Dinamita, Durango	M	81				
CMN42	Viesca, Coahuila	M	88				

Information of locality, sex and SVL of individual samples of venoms from *C. basiliscus* (CBA), *C. m. molossus* (CMM), *C. m nigrescens* (CMN), *C. m. oaxacus* (CMO), and *C. ornatus* (CO). SVL: snout-vent length. Snakes were sorted by SVL from smallest to largest.

2.4. Electrophoretic profiles

The electrophoretic profile of individual venoms (20 μg) was determined by 12.5 % or 15 % SDS-PAGE under reducing conditions as previously described in detail (Borja et al., 2018b). Proteins were stained with Coomassie blue. Electrophoretic profile differences between smaller and larger individuals were used to classify venoms as "juvenile" and "adult" and prepare the venom pools (Section 2.3).

2.5. Proteomic profiling of venoms

(a) '*Snake venomics*': the analytical strategy developed by Calvete et al. (2007) was used to determine protein family composition and to estimate relative abundances. We selected venom from small and large individuals of each of the five lineages, with different electrophoretic profiles. Although we did not obtain venom proteomes from representative large individuals of *C. m. nigrescens* (SVL: 81 cm) and *C. m. oaxacus* (SVL:89 cm), we used the RP-HPLC chromatograms of whole venoms and SDS-PAGE profiles of RP-HPLC fractions to estimate the abundance of the major toxin families in two representative individuals (CMN46 and CMO03). Three milligrams (mg) of venom were dissolved in 0.4 mL of 0.1 % trifluoroacetic acid and fractionated on a C_{18} analytical column (Agilent, 250 × 4.6 mm) using an Agilent 1100 chromatograph monitored at 214 nm. Solution A (0.1 % TFA in water) and solution B (0.1 % TFA in acetonitrile 99.9 %) were used to generate an elution gradient (5 % B for 5 min, followed 5–15 % B for 10 min, 15–45 % B for 60 min, 45–70 % B for 12 min, and B 100 % for 10 min) at 1 mL/min (Neri-Castro et al., 2022). Fractions were manually collected, dried in a SpeedVac centrifuge, and then redissolved in 20–50 μL of water (depending on the fraction abundance) for subsequent separation by 12.5 % SDS-PAGE (Supplementary Figs. S1–S5). Coomassie-stained protein bands were excised and subjected to in-gel reduction (10 mM dithiothreitol), alkylation (50 mM iodacetamide), and overnight digestion with sequencing grade bovine trypsin (in 25 mM ammonium bicarbonate) using an automated workstation (Intavis). The resulting peptides were analyzed by nano-LC-MS/MS in a Q-Exactive Plus (Thermo-Fisher) mass spectrometer under previously described conditions (Neri-Castro et al., 2022). Five μL of each tryptic digest were loaded on a C_{18} trap column (75 μm × 2 cm, 3 μm particle; PepMap, Thermo), washed with 0.1 % formic acid (solution A), and separated at 200 nL/min with a 3 μm particle, 15 cm × 75 μm C_{18} Easy-spray® analytical column using a nano-Easy® 1200 chromatograph (Thermo-Fisher). A gradient from 0.1 % formic acid (solution A) to 80 % acetonitrile with 0.1 % formic acid (solution B) was developed: 1–5 % B in 1 min, 5–25 % B in 30 min, 25–79 % B in 6 min, 79–99 % B in 2 min, and 99 % B in 6 min, for a total time of 45 min. MS spectra were acquired in positive mode at 1.9 kV, with a capillary temperature of 200 °C, using 1 scan at 400–1600 *m/z*, maximum injection time of 100 ms, AGC target of 3×10^6, and orbitrap resolution of 70,000. The top 10 ions with 2–5 positive charges were fragmented with AGC target of 1×10^5, maximum injection time of 110 ms, resolution 17,500, loop count 10, isolation window of 1.4 *m/z*, and a dynamic exclusion time of 5 s. MS/MS spectra were processed to assign peptide matches to known protein families by similarity with sequences in the UniProt/SwissProt database (Serpentes) using Peaks X® (Bioinformatics Solutions). Cysteine carbamidomethylation was set as a fixed modification, while deamidation of asparagine or glutamine, and methionine oxidation were set as variable modifications, allowing up to 3 missed

cleavages by trypsin. Parameters for match acceptance were set to FDR < 1 %, −10lgP protein score ≥30, unique peptides ≥1. Each toxin family's relative abundance (expressed as a percentage of the total venom proteins) was estimated from the relation of the sum of the areas of the reverse-phase chromatographic peaks to the total area of venom protein peaks in the reverse-phase chromatogram. When more than one protein band appeared in SDS-PAGE, their proportions were estimated by densitometry, using ImageLab software (Bio-Rad). Protein family abundances were expressed as percentages and represented in pie charts (Calvete et al., 2007).

'*Snake venomics*': the analytical strategy developed by Calvete et al. (2007) was used to determine protein family composition and to estimate relative abundances. We selected venom from small and large individuals of each of the five lineages, with different electrophoretic profiles. Although we did not obtain venom proteomes from representative large individuals of *C. m. nigrescens* (SVL: 81 cm) and *C. m. oaxacus* (SVL: 89 cm), we used the RP-HPLC chromatograms of whole venoms and SDS-PAGE profiles of RP-HPLC fractions to estimate the abundance of the major toxin families in two representative individuals (CMN46 and CMO03). Three milligrams (mg) of venom were dissolved in 0.4 mL of 0.1 % trifluoroacetic acid and fractionated on a C_{18} analytical column (Agilent, 250 × 4.6 mm) using an Agilent 1100 chromatograph monitored at 214 nm. Solution A (0.1 % TFA in water) and solution B (0.1 % TFA in acetonitrile 99.9 %) were used to generate an elution gradient (5 % B for 5 min, followed 5–15 % B for 10 min, 15–45 % B for 60 min, 45–70 % B for 12 min, and B 100 % for 10 min) at 1 mL/min (Neri-Castro et al., 2022). Fractions were manually collected, dried in a SpeedVac centrifuge, and then redissolved in 20–50 μL of water (depending on the fraction abundance) for subsequent separation by 12.5 % SDS-PAGE (Supplementary Figs. S1–S5). Coomassie-stained protein bands were excised and subjected to in-gel reduction (10 mM dithiothreitol), alkylation (50 mM iodacetamide), and overnight digestion with sequencing grade bovine trypsin (in 25 mM ammonium bicarbonate) using an automated workstation (Intavis). The resulting peptides were analyzed by nano-LC-MS/MS in a Q-Exactive Plus (Thermo-Fisher) mass spectrometer under previously described conditions (Neri-Castro et al., 2022). Five μL of each tryptic digest were loaded on a C_{18} trap column (75 μm × 2 cm, 3 μm particle; PepMap, Thermo), washed with 0.1 % formic acid (solution A), and separated at 200 nL/min with a 3 μm particle, 15 cm × 75 μm C_{18} Easy-spray® analytical column using a nano-Easy® 1200 chromatograph (Thermo-Fisher). A gradient from 0.1 % formic acid (solution A) to 80 % acetonitrile with 0.1 % formic acid (solution B) was developed: 1–5 % B in 1 min, 5–25 % B in 30 min, 25–79 % B in 6 min, 79–99 % B in 2 min, and 99 % B in 6 min, for a total time of 45 min. MS spectra were acquired in positive mode at 1.9 kV, with a capillary temperature of 200 °C, using 1 scan at 400–1600 *m/z*, maximum injection time of 100 ms, AGC target of 3×10^6, and orbitrap resolution of 70,000. The top 10 ions with 2–5 positive charges were fragmented with AGC target of 1×10^5, maximum injection time of 110 ms, resolution 17,500, loop count 10, isolation window of 1.4 *m/z*, and a dynamic exclusion time of 5 s. MS/MS spectra were processed to assign peptide matches to known protein families by similarity with sequences in the UniProt/SwissProt database (Serpentes) using Peaks X® (Bioinformatics Solutions). Cysteine carbamidomethylation was set as a fixed modification, while deamidation of asparagine or glutamine, and methionine oxidation were set as variable modifications, allowing up to 3 missed cleavages by trypsin. Parameters for match acceptance were set to FDR < 1 %, −10lgP protein score ≥30, unique peptides ≥1. Each toxin family's relative abundance (expressed as a percentage of the total venom proteins) was estimated from the relation of the sum of the areas of the reverse-phase chromatographic peaks to the total area of venom protein peaks in the reverse-phase chromatogram. When more than one protein band appeared in SDS-PAGE, their proportions were estimated by densitometry, using ImageLab software (Bio-Rad). Protein family abundances were expressed as percentages and represented in pie charts (Calvete et al., 2007).

(b) '*Shotgun*' *proteomic profiling*: To determine the number and identity of venom toxins, we followed the methods outlined by Smith et al. (2023). Lyophilized venoms representative of the five lineages were redissolved in 8 M urea/0.1 M Tris (pH 8.5), and disulfide bonds were reduced with 5 mM TCEP (tris(2-carboxyethyl)phosphine) for 20 min, followed by alkylation with 50 mM 2-chloro-2-iodacetamide for 15 min in the dark, all at room temperature. Samples were diluted with four volumes of 100 mM Tris-HCl (pH 8.5), and digested with sequencing grade trypsin (Promega) at an enzyme/substrate ratio of 1:20 overnight at 37 °C. Following the overnight digestion, formic acid (FA) was added to the samples to a final concentration of 5 %, and tryptic peptides were purified with C_{18} ZipTips (Millipore, Billerica, MA) following the manufacturer's protocol. Digests were dried in a vacuum centrifuge and redissolved in 0.1 % FA. Liquid chromatography-tandem mass spectrometry (LC–MS/MS) was conducted using an Easy nLC 1000 instrument coupled with a Q Exactive HF Mass Spectrometer, both from ThermoFisher Scientific. For each venom sample, 3 μg of digested peptides were applied to a C_{18} column (100 μm inner diameter × 20 cm) packed in-house with 2.7 μm Cortecs C_{18} resin. The peptides were separated at a flow rate of 0.4 μl/min with solution A (0.1 % FA) and solution B (0.1 % FA in ACN) under the following conditions: isocratic at 4 % solvent B for 3 min, followed by a gradient from 4 % to 32 % solvent B over 102 min, then 32 % to 55 % solvent B over 5 min, 55 % to 95 % solvent B over 1 min, and isocratic at 95 % solvent B for 9 min. Mass spectrometry was performed in data-dependent acquisition (DDA) mode. Full MS scans were conducted from *m/z* 300 to 1800 with a resolution of 60,000, an automatic gain control (AGC) target of 1×10^6, and a maximum injection time (IT) of 50 ms. The top 15 most abundant precursors, exceeding an intensity threshold of 9.1×10^3 were selected for MS/MS acquisition with a resolution of 15,000, 1×10^5 AGC, and a maximal IT of 110 ms. The isolation window was set to 2.0 *m/z* and ions were fragmented at a normalized collision energy of 30. Dynamic exclusion was applied for 20 s.

Fragmentation spectra were searched against the venom gland transcriptomes of individuals from the five lineages from the *C. molossus* complex (data in preparation) using the MSFragger-based FragPipe computational platform (Kong et al., 2017). Contaminants and reverse decoys were added to the database automatically. The precursor-ion mass tolerance and fragment-ion mass tolerance were set to 15 and 20 ppm, respectively. Fixed modifications were set as carbamidomethyl (C), and variable modifications were set as oxidation (M), two missed tryptic cleavages were allowed, and the protein-level false discovery rate (FDR) was ≤1 %. The relative abundance of major toxin families was compared across samples using total spectral intensity.

We used the R package 'pheatmap' to generate heatmaps to visualize better differences in protein family abundances across individual venoms within each lineage. These heatmaps display the summed spectral intensities of each protein family (Figs. 2–6).

2.6. Mass spectrometry (ESI-MS)

Intact masses of specific venom components were determined in a Finnigan LCQFleet mass spectrometer (Thermo) with electrospray ionization (ESI-MS). Samples were analyzed in positive ionization mode

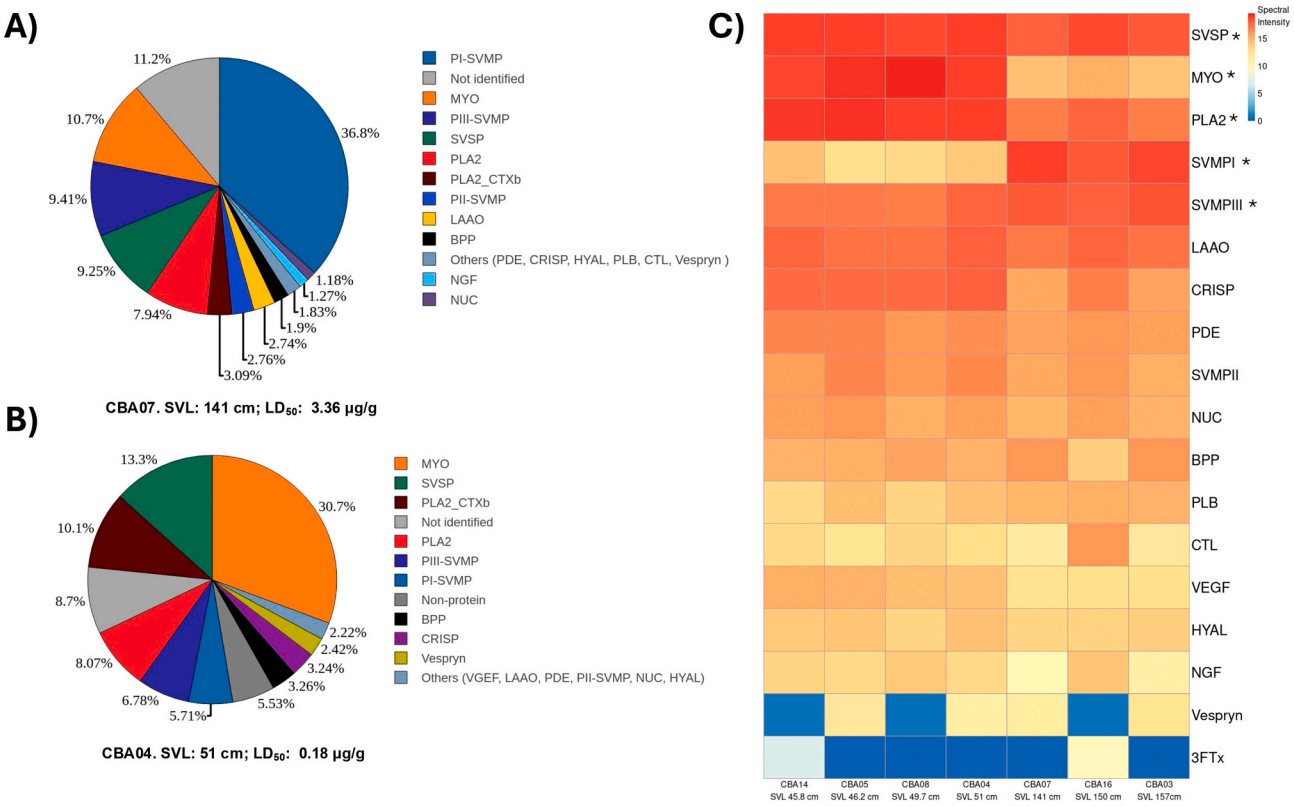

Fig. 2. Proteomic profiling of venoms from *C. basiliscus* using 'snake venomics' (A and B) and shotgun (C) strategies. Venom proteins from large (A) and small (B) representative individuals of *C. basiliscus* were fractionated on a C_{18} column. HPLC fractions were further separated by 12.5 % SDS-PAGE under reducing conditions. The identity of toxins was determined by LC-MS/MS in both venoms. The abundance of toxins was estimated via the area under the curve of RP-HPLC fractions and densitometry of SDS-PAGE bands. The pie charts depict the relative abundance of each toxin family/subfamily in the venom. (C) Heatmap showing the summed spectral intensities of proteins per protein family and subfamily in *C. basiliscus* venoms obtained by shotgun proteomics. The heatmap of toxins is ordered from greatest to least average spectral intensity, with warmer colors indicating higher abundance. Individuals are sorted from smallest to largest. The asterisk indicates a significant relationship between the protein family spectral intensity and individual SVL. 3FTx, three-finger toxins; BPP, bradykinin-potentiating-like peptides; CRISP, cysteine-rich secretory protein; CTL, C-type lectin/lectin like; CTXb, crotoxin subunit B; HYAL, hyaluronidase; LAAO, L-amino acid oxidase; MYO, myotoxin-*a*/crotamine; NGF, nerve growth factors; NUC, 5′ nucleotidase; PDE, phosphodiesterase; PLA_2, phospholipase A_2; PLB, phospholipase B; SVMP, snake venom metalloproteinase; SVSP, snake venom serine protease; VEGF, Vascular endothelial growth factor. Not identified: RP-HPLC fractions not identified by LC-MS/MS. Non-protein: No bands were observed by SDS-PAGE.

by direct infusion at 10 µL/min and spray voltage of 1.9 kV, using 50 % acetonitrile and 0.1 % acetic acid as solvent. Spectra were acquired using the Tune Plus software (Thermo) and deconvolution was performed with Xtract software (Walzthoeni et al., 2015) to obtain isotope-averaged intact molecular masses (Neri-Castro et al., 2022).

2.7. Chromatographic profiles by RP-HPLC of individual and pooled venoms

To compare the chromatographic profile of venoms, 1 mg of individual venoms or 0.5 mg of pooled venoms were fractionated by RP-HPLC as described in the prior Section 2.5. Using the area under the curve, we estimated the relative abundance of the fractions predominantly containing SVMP and MYO, based on reference venom proteomes.

2.8. Proteolytic activity

The proteolytic activity was assessed using azocasein (Sigma-Aldrich, St. Louis, MO, USA) as substrate, following Colis-Torres et al. (2022). An azocasein solution was prepared dissolving azocasein in buffer (50 mM Tris-HCl, 0.15 M NaCl, and 25 mM $CaCl_2$, pH 8.0) in a final concentration of 10 mg/mL. Then, 20 µg of each venom was added to 100 µL of azocasein solution and incubated for 30 min at 37 °C. After that, 200 µL of 5 % trichloroacetic acid was added to the mixture and centrifuged at 13,000 rpm for 5 min. Then, 150 µL of the supernatant was added to 150 µL of 0.5 M NaOH in a 96-well plate. Sample absorbance was measured at 450 nm (Wang et al., 2004). Each venom sample was assessed in triplicate. One unit of proteolytic activity was defined as a change of 0.2 in absorbance per min.

2.9. Phospholipase A_2 activity

The synthetic substrate 4-nitro-3-(octanoyloxy)-benzoic acid (4-NOBA) was used to determine the PLA_2 activity of individual venoms (Holzer and Mackessy, 1996). Microplate wells were filled with 200 µL of reaction buffer (10 mM Tris, 10 mM CaCl2, 0.1 M NaCl, pH 8.0) and 25 µL of the substrate (4-NOBA; 1 mg/mL acetonitrile). The reaction buffer and substrate were incubated at 37 °C for 10 min and then 20 µL of venom (1 mg/mL) was added. The mixture was incubated at 37 °C for 40 min, and the absorbance was measured at 450 nm. The raw values were multiplied by 10 (arbitrary value) for better visualization. Each sample was analyzed in triplicate.

2.10. Fibrinogenolytic activity

To evaluate the fibrinogenolytic activity, human fibrinogen (50 µg) was incubated with representative venoms (10 µg) of small and large snakes from the five lineages in a final volume of 50 µL of PBS for 30 min at 37 °C (Zarzosa et al., 2023). Then, 10 µL of the mixture was separated

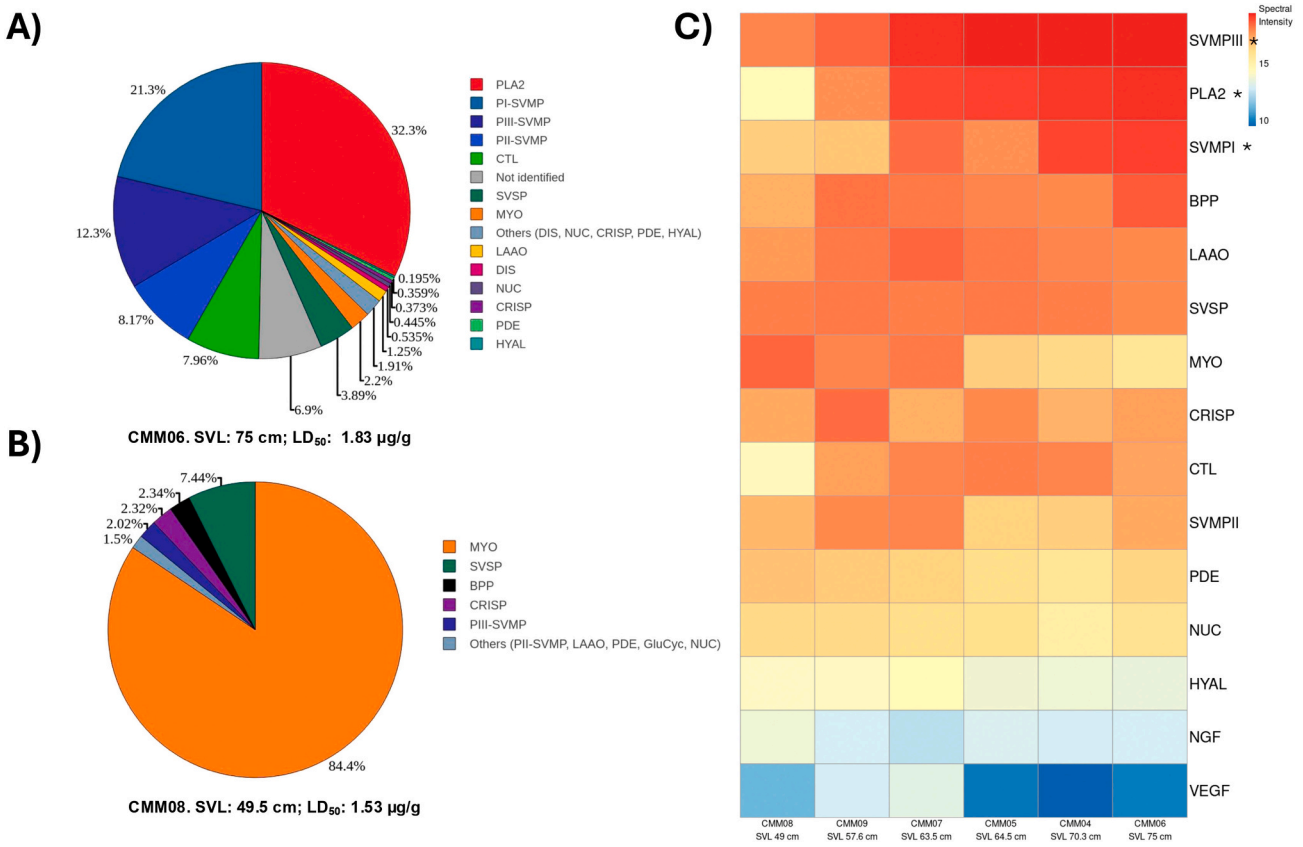

Fig. 3. Proteomic profiling of venoms from *C. m. molossus* using 'snake venomics' (A and B) and shotgun (C) strategies. Venom proteins from large (A) and small (B) representative individuals of *C. m. molossus* were fractionated on a C_{18} column. RP-HPLC fractions were further separated by 12.5 % SDS-PAGE under reducing conditions. The identity of toxins was determined by LC-MS/MS in both venoms. The abundance of toxins was estimated via the area under the curve of RP-HPLC fractions and densitometry of SDS-PAGE bands. The pie charts depict the relative abundance of each toxin family/subfamily in the venom. (C) Heatmap showing the summed spectral intensities of proteins per protein family and subfamily in *C. m. molossus* venoms obtained by shotgun proteomics. The heatmap of toxins is ordered from greatest to least average spectral intensity, with warmer colors indicating higher abundance. Individuals are sorted from smallest to largest. The asterisk indicates a significant relationship between the protein family spectral intensity and individual SVL. BPP, bradykinin-potentiating-like peptides; DIS, disintegrin; CRISP, cysteine-rich secretory protein; CTL, C-type lectin/lectin-like; HYAL, hyaluronidase; LAAO, L-amino acid oxidase; MYO, myotoxin-*α*/crotamine; NGF, nerve growth factors; NUC, 5′ nucleotidase; PDE, phosphodiesterase; PLA_2, phospholipase A_2; SVMP, snake venom metalloproteinase; SVSP, snake venom serine protease; VEGF, Vascular endothelial growth factor. Not identified: RP-HPLC fractions not identified by LC-MS/MS. Non-protein: No bands were observed by SDS-PAGE.

by 12.5 % SDS-PAGE under reducing conditions. To evaluate the contribution of SVMPs and SVSPs to the fibrinogenolytic activity of venoms, additional experiments preincubating venoms with SVMP and SVSP inhibitors (5 mM EDTA and 5 mM PMSF, respectively) for 30 min at 37 °C were carried out as above. Fibrinogen without venom was used as a control.

2.11. Lethality (LD_{50}) of individual and pooled venoms

The venom lethality (median lethal dose, LD_{50}) of representative small and large snakes from the five lineages were evaluated both individually and in pooled samples, as previously described (Borja et al., 2018a, 2018b). Groups of three ICR mice (18–20 g) were intravenously (i.v.) injected via the caudal vein with different amounts of venom dissolved in 0.2 mL of phosphate buffer solution (PBS), pH 7.2. Insulin syringes of 1 mL capacity with 31G needles were used. The percentage of dead mice 24 h after inoculation was plotted against the logarithm of the quantity of venom injected. LD_{50} values were estimated by non-linear regression using GraphPad Prism V.10 (GraphPad Software, La Jolla, CA, USA, 2005) (Lorke, 1983).

Additionally, to assess the lethality of venoms with varying compositions against different potential prey, we determined the intraperitoneal (i.p.) LD_{50} of venom from two *C. m. nigrescens* (CMN40 and CMN46) and one *C. m. oaxacus* (CMO03) in both a mammalian (mouse) model and a reptilian (black iguana) model. Different amounts of venom were injected into groups of three mice and groups of three black iguanas, in a final volume of 0.2 mL of PBS. The solution was administered using 1 mL syringes. The percentage of deceased animals was recorded 24 h after injection, and the LD_{50} was estimated as previously described.

2.12. Neutralization of lethal activity by Antivipmyn®

Amounts equivalent to 3 × LD_{50} of juvenile or adult venom pools from the five lineages of the *C. molossus* complex were incubated with different volumes of Antivipmyn® for 30 min at 37 °C. The preincubated mixtures (0.2 mL) were injected intravenously into groups of three CD-1 mice weighing 18–20 g. The number of dead mice after 24 h was counted for each experimental group. The percentage of survival was plotted as a function of the logarithm of antivenom volume using the non-linear sigmoid dose-response regression method in the GraphPad Prism software (V.10). The ED_{50} was expressed as µL of antivenom required to neutralize 3 × LD_{50} of venom and as milligrams of antivenom that neutralizes 1 mg of venom (Gutiérrez et al., 2017b).

2.13. Immunorecognition of whole venoms by Antivipmyn®

ELISA was used to evaluate the immunorecognition of juvenile and adult pool venoms of the five lineages by Antivipmyn® following the

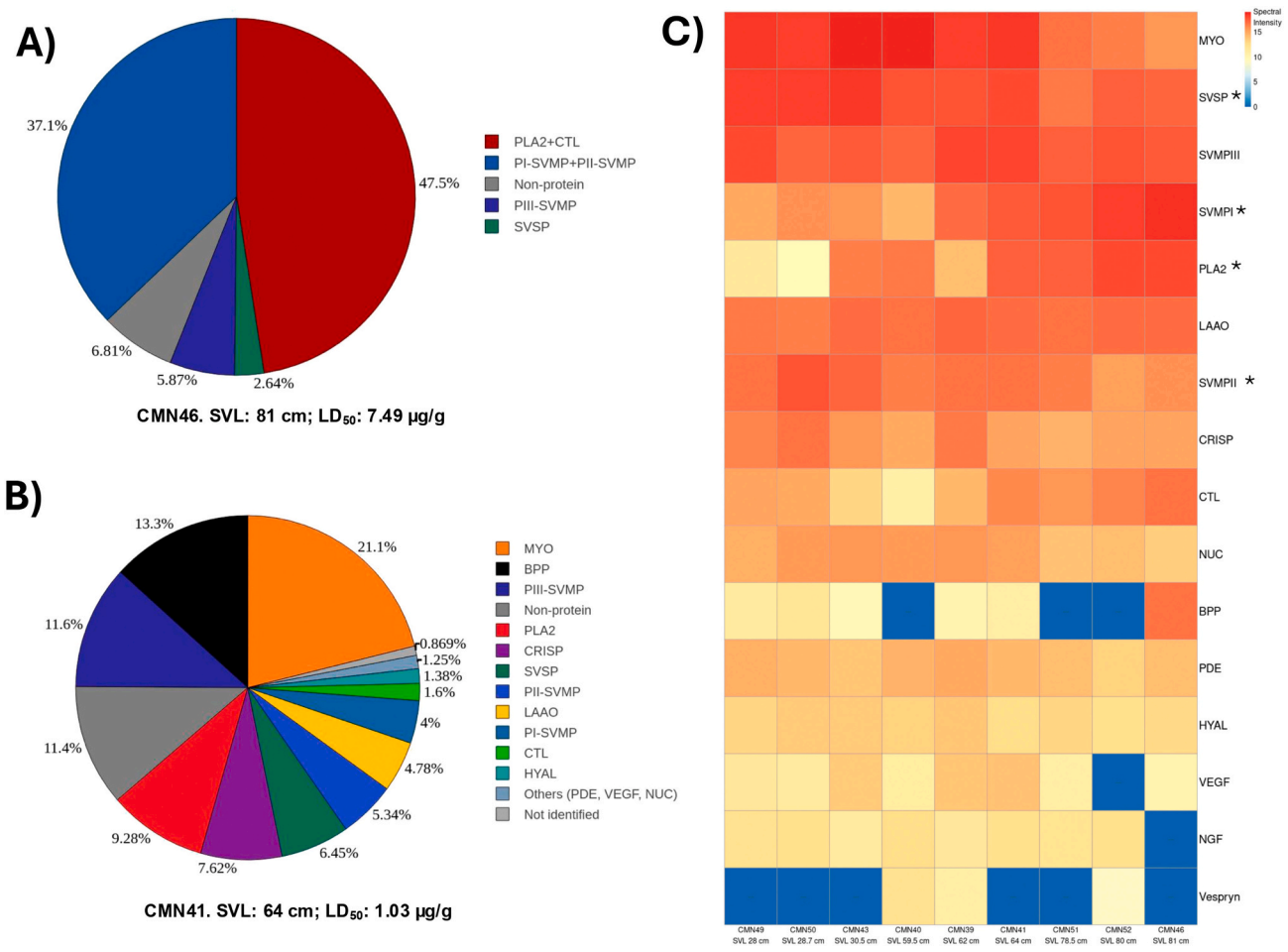

Fig. 4. Proteomic profiling of venoms from *C. m. nigrescens* using the RP-HPLC and SDS-PAGE profiles (A), 'snake venomics' (B), and shotgun (C) strategies. Venom proteins from a large (A) and small (B) representative individual of *C. m. nigrescens* were fractionated on a C_{18} column. HPLC fractions were further separated by 12.5 % SDS-PAGE under reducing conditions. The identity of toxins was estimated by RP-HPLC and SDS-PAGE profiles and ESI-MS masses (A) or determined by LC-MS/MS (B). The abundance of toxins was calculated via the area under the curve of RP-HPLC fractions and densitometry of SDS-PAGE bands. The pie charts depict the relative abundance of each toxin family/subfamily in the venom. Due to the similar molecular masses and elution times of PLA_2/CTL and PI-SVMP/PII-SVMP, we could not distinguish between them in the venom of the large individual (A). As a result, their abundance was expressed as PLA_2 + CTL and PI+PII-SVMP. (C) Heatmap showing the summed spectral intensities of proteins per protein family and subfamily in *C. m. nigrescens* venoms obtained by shotgun proteomics. The heatmap of toxins is ordered from greatest to least average spectral intensity, with warmer colors indicating higher abundance. Individuals are sorted from smallest to largest. The asterisk indicates a significant relationship between the protein family spectral intensity and individual SVL. BPP, bradykinin-potentiating-like peptides; DIS, disintegrin; CRISP, cysteine-rich secretory protein; CTL, C-type lectin/lectin-like; HYAL, hyaluronidase; LAAO, L-amino acid oxidase; MYO, myotoxin-*a*/crotamine; NGF, nerve growth factors; NUC, 5′ nucleotidase; PDE, phosphodiesterase; PLA_2, phospholipase A_2; SVMP, snake venom metalloproteinase; SVSP, snake venom serine protease; VEGF, Vascular endothelial growth factor. Not identified: RP-HPLC fractions not identified by LC-MS/MS. Non-protein: No bands were observed by SDS-PAGE.

protocol described by (Ponce-López et al., 2021, 2020). A hundred microliters of venom (5 µg/mL) dissolved in coating buffer (100 mM $NaHCO_3$, pH 9.5) were added to ELISA plates (SPL Life Sciences) with 96 wells. After 1 h of incubation at 37 °C, the plate was rinsed (50 mM Tris-HCl, pH 8, 150 mM NaCl, 0.02 % Tween 20), and 200 µL of blocking solution (50 mM Tris-HCl, pH 8, 5 mg/mL gelatin, 0.02 % Tween 20) were added in each well. After overnight incubation at 4 °C, the plate was washed. Then, 100 µL of 700 µg/mL of Antivipmyn® were placed in the first well, followed by serial 1:3 dilutions in working buffer (50 mM Tris-HCl pH 8, 0.5 M NaCl, 0.1 % gelatin, 0.05 % of Tween 20). After 1 h of incubation at 37 °C, the plate was washed, and 100 µL of goat anti-horse IgG conjugated to horseradish peroxidase was added to each well at a dilution of 1: 3000 in a working buffer to incubate again at 37 °C for 1 h. Finally, after washing, 100 µL of revealing buffer (ABTS solution, Roche®) was added, and after 15 min at room temperature, the absorbance at 405 nm was measured using a spectrophotometer (Magellan®). ELISA results were analyzed by plotting a sigmoidal dose-response curve in the GraphPad Prism software (V.10) to obtain the antibody titer EC_{50}, defined as the concentration (mg/mL) of antivenom resulting in half-maximal ELISA signal.

2.14. Partial isolation of lethal components in the CMO08 venom (C. m. oaxacus)

To identify the toxin(s) responsible for the low LD_{50} of CMO08 venom, this venom (43 mg) was fractionated by gel filtration on a Sephadex G-75 column. The resulting four fractions were evaluated for lethality by injecting intravenously 25 µg of each fraction into three CD-1 mice weighing 18–20 g. After 24 h, only fraction 1 (F1) was able to kill the three injected mice, whereas the remaining fractions did not kill any mice. LD_{50} of F1 was calculated as previously described. F1 was further separated by RP-HPLC and SDS-PAGE to identify toxin families responsible for lethality based on the retention time of RP-HPLC fractions and the molecular mass of SDS-PAGE bands.

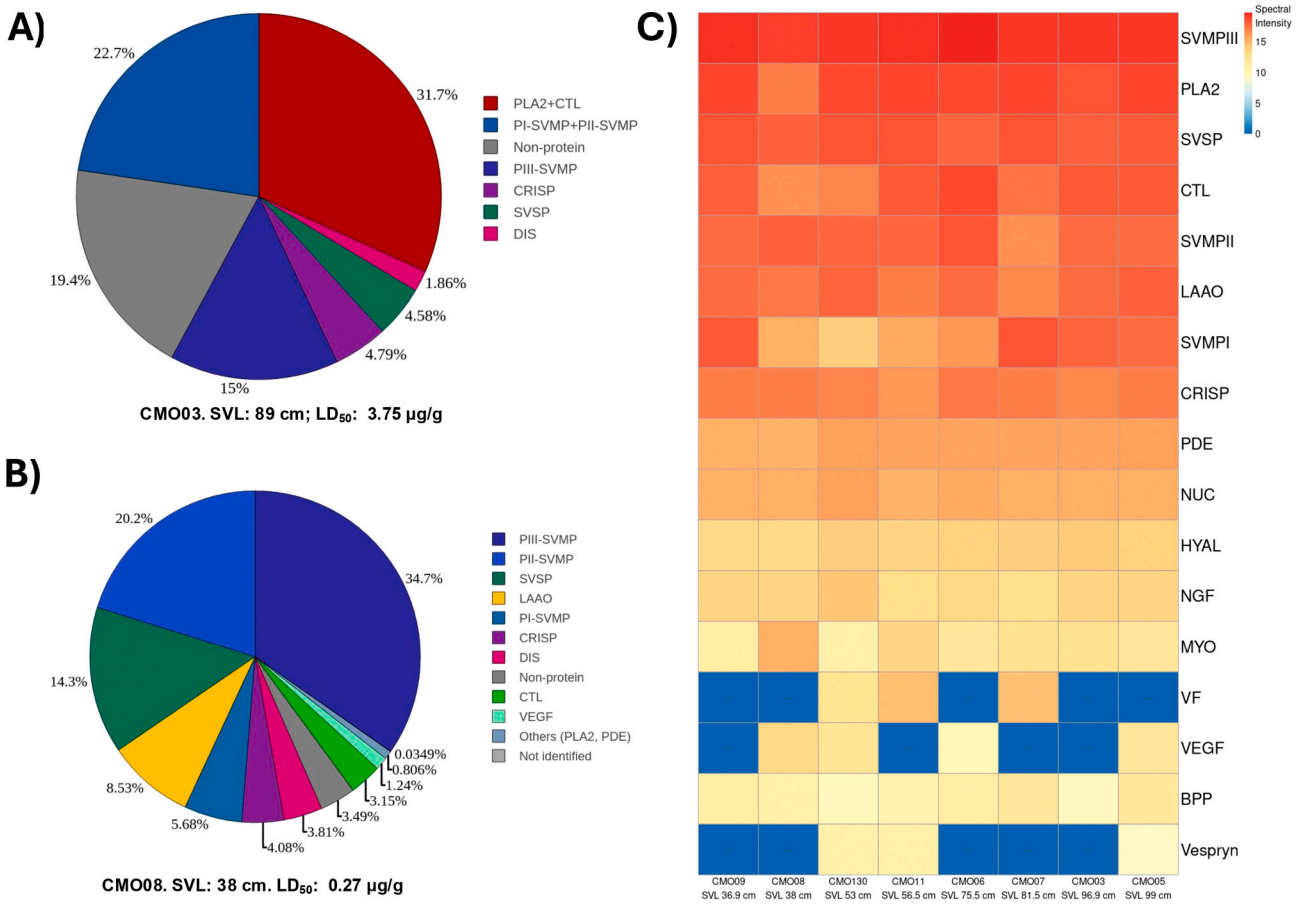

Fig. 5. Proteomic profiling of venoms from *C. m. oaxacus* using the RP-HPLC and SDS-PAGE profiles (A), 'snake venomics' (B), and shotgun (C) strategies. Venom proteins from a large (A) and small (B) representative individual of *C. m. oaxacus* were fractionated on a C_{18} column. HPLC fractions were further separated by 12.5 % SDS-PAGE under reducing conditions. The identity of toxins was estimated by RP-HPLC and SDS-PAGE profiles and ESI-MS masses (A) or determined by LC-MS/MS (B). The abundance of toxins was calculated via the area under the curve of RP-HPLC fractions and densitometry of SDS-PAGE bands. The pie charts depict the relative abundance of each toxin family/subfamily in the venom. Due to the similar molecular masses and elution times of PLA_2/CTL and PI-SVMP/PII-SVMP, we could not distinguish between them in the venom of the large individual (A). As a result, their abundance was expressed as PLA_2 + CTL and PI+PII-SVMP. (C) Heatmap showing the summed spectral intensities of proteins per protein family and subfamily in *C. m. oaxacus* venoms obtained by shotgun proteomics. The heatmap of toxins is ordered from greatest to least average spectral intensity, with warmer colors indicating higher abundance. Individuals are sorted from smallest to largest. BPP, bradykinin-potentiating-like peptides; DIS, disintegrin; CRISP, cysteine-rich secretory protein; CTL, C-type lectin/lectin-like; HYAL, hyaluronidase; LAAO, L-amino acid oxidase; MYO, myotoxin-*a*/crotamine; NGF, nerve growth factors; NUC, 5′ nucleotidase; PDE, phosphodiesterase; PLA_2, phospholipase A_2; SVMP, snake venom metalloproteinase; SVSP, snake venom serine protease; VEGF, Vascular endothelial growth factor. Not identified: RP-HPLC fractions not identified by LC-MS/MS. Non-protein: No bands were observed by SDS-PAGE.

2.15. Statistical analysis

Depending on whether the normality test failed or not, one-way ANOVA or one-way ANOVA on ranks was carried out using the program Sigma Plot®11 to determine significant ($p < 0.05$) differences in the proteolytic activity, phospholipase A_2 activity, and LD_{50} among the five lineages. We carried out linear regressions using as dependent variables the abundance of MYO, PLA_2, SVMP, PI-SVMP, PII-SVMP, PIII-SVMP, and SVSP estimated from shotgun proteomics (spectral intensities) and RP-HPLC chromatograms (area percentages) and as independent variable SVL. Before performing the regression analysis, we transformed the area percentages of toxin families, obtained from areas under peaks of chromatograms, from percentages to arcs in square root values. We also regressed the proteolytic and phospholipase activities of the venoms to SVL of the snakes from the five snake lineages.

3. Results

3.1. Snake venomics of representative individuals of the C. molossus complex

Venom composition was obtained by first fractionating the venom using RP-HPLC, followed by further separation of the RP-HPLC fractions via SDS-PAGE. Tryptic peptides derived by in-gel digestion of Coomassie Blue-stained SDS-PAGE bands were identified using nano-LC-MS/MS. The four most abundant toxin families across the ten representative venom proteomes were PLA_2, MYO, SVMP, and SVSP, comprising between 0 % and 84.5 % of the total proteins. Moderately abundant toxin families (0 to 15 %) included bradykinin-potentiating-like peptides (BPP), cysteine-rich secretory protein (CRISP), C-type lectin/lectin-like (CTL), and L-amino acid oxidase (LAAO). Low abundant toxin families (0 to 5 %) included disintegrin (DIS), hyaluronidase (HYAL), nerve growth factor (NGF), 5′ nucleotidase (NUC), phospholipase B (PLB), phosphodiesterase (PDE), vascular endothelial growth factor (VEGF), and Vespryn (Figs. 2–6, Supplementary Tables S1–S8).

For the larger *C. basiliscus* (CBA07; SVL: 141 cm), the venom

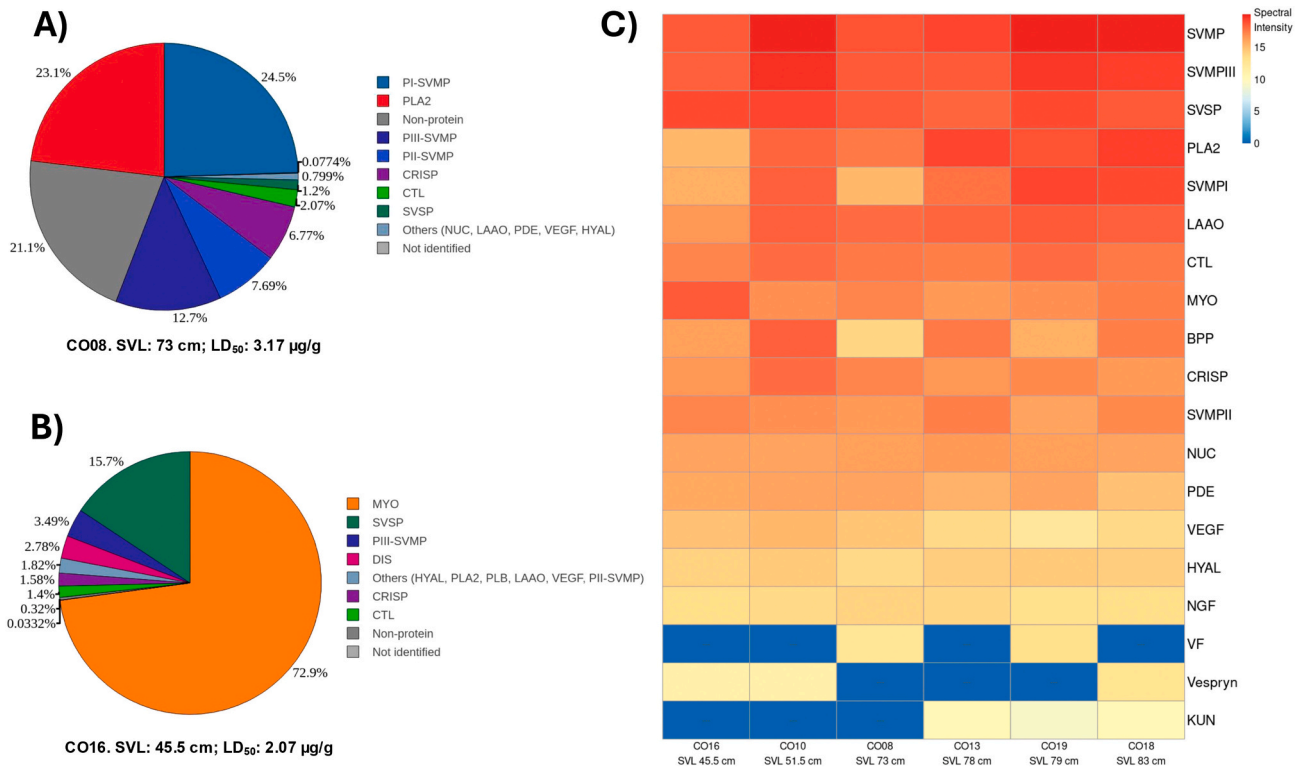

Fig. 6. Proteomic profiling of venoms from *C. ornatus* using 'snake venomics' (A and B) and shotgun (C) strategies. Venom proteins from a large (A) and small (B) representative individual of *C. ornatus* were fractionated on a C_{18} column. HPLC fractions were further separated by 12.5 % SDS-PAGE under reducing conditions. The identity of toxins was determined by LC-MS/MS in both venoms. The abundance of toxins was estimated via the area under the curve of RP-HPLC fractions and densitometry of SDS-PAGE bands. The pie charts depict the relative abundance of each toxin family/subfamily in the venom. (C) Heatmap showing the summed spectral intensities of proteins per protein family and subfamily in *C. ornatus* venoms obtained by shotgun proteomics. The heatmap of toxins is ordered from greatest to least average spectral intensity, with warmer colors indicating higher abundance. Individuals are sorted from smallest to largest. BPP, bradykinin-potentiating-like peptides; DIS, disintegrin; CRISP, cysteine-rich secretory protein; CTL, C-type lectin/lectin-like; HYAL, hyaluronidase; KUN, Kunitz peptide LAAO, L-amino acid oxidase; MYO, myotoxin-*a*/crotamine; NUC, 5′ nucleotidase; PDE, phosphodiesterase; PLA_2, phospholipase A_2; SVMP, snake venom metalloproteinase; SVSP, snake venom serine protease; VEGF, Vascular endothelial growth factor; VF, Venom factor. Not identified: RP-HPLC fractions not identified by LC-MS/MS. Non-protein: No bands were observed by SDS-PAGE.

proteome was dominated by SVMPs (36.8 % PI-SVMP, 9.4 % PIII-SVMP, and 2.8 % PII-SVMP), with other notable toxin families including MYO (10.7 %), PLA_2 (11 %), and SVSP (9.3 %). In contrast, the venom of the smaller *C. basiliscus* (CBA04; SVL: 51 cm) was primarily composed of MYO (30.7 %), PLA_2 (18.2 %), and SVSP (13.3.%) (Fig. 2A and B, Supplementary Tables S1–S8). The basic subunit of CTX, crotoxin B, made up 3.1 % and 10.1 % of the venom proteomes of CBA07 and CBA04, respectively.

In the venom of the larger *C. m. molossus* (CMM06; SVL: 75 cm), the three most abundant toxin families were SVMPs (41.8 %), PLA_2s (32.3 %), and CTLs (8.0 %), with PI-SVMP being the most prevalent SVMP (21.3 %). Less abundant toxin families in CMM06 included SVSP (3.9 %) and MYO (2.2 %). Surprisingly, the venom of the smaller *C. m. molossus* (CMM08; SVL: 45 cm) was predominantly MYO (84.4 %), with SVSP as the second most abundant component (7.4 %) (Fig. 3A and B, Supplementary Tables S1–S8).

For the smaller *C. m. nigrescens* (CMN41; SVL: 64 cm), the predominant toxin families were MYO (21.1 %), SVMP (11.6 % PIII-SVMP, 5.3 % PII-SVMP, and 4.0 % PI-SVMP), and BPPs (13.3 %). Other relatively abundant toxin families included PLA_2 (9.3 %), CRISP (7.6 %), SVSP (6.4 %), and LAAO (4.8 %) (Fig. 4B, Supplementary Tables S1–S8).

The venom of the smaller *C. m. oaxacus* (CMO08; SVL: 38 cm) was largely composed of SVMPs (60.6 %), with the PIII subclass being the most abundant (34.7 %), followed by PII (20.2 %) and PI (5.7 %). The second and third most abundant toxin families in CMO08 were SVSP and LAAO, with a relative abundance of 14.3 % and 8.5 %, respectively (Fig. 5B, Supplementary Tables S1–S8).

For the larger *C. ornatus* (CO08; SVL: 73 cm), SVMPs made up 44.9 % of the venom proteome (24.5 % PI-SVMP, 7.7 % PII-SVMP, 12.7 % PIII-SVMP), followed by PLA_2 (23.1 %), and CRISP (6.8 %). In contrast, the venom of the smaller *C. ornatus* (CO16; SVL: 45.5 cm) was dominated by MYO (72.9 %), with SVSP (15.7 %), and SVMPs (PIII-SVMP 3.5 % and PII-SVMP 0.7 %) as second and third most abundant components, respectively (Fig. 6A and B, Supplementary Tables S1–S8).

Although we did not confirm the identity of toxins by mass spectrometry for venoms from two representative adult individuals of *C. m. nigrescens* (CMN46) and *C. m. oaxacus* (CMO03), we estimated the abundance of dominant toxin families in both venoms based on (1) the elution times and molecular masses of peaks in RP-HPLC chromatograms, and (2) molecular mass of SDS-PAGE bands corresponding to each RP-HPLC peak. PLA_2 + CTL (47.5 %), PI-SVMP+PII-SVMP (37.1 %), PIII-SVMP (5.9 %), and SVSP (2.6 %) made up the most abundant toxin families in CMN46 venom (Fig. 4A). On the other hand, the composition of CMO03 venom was predominantly made up of PLA_2 + CTL (31.7 %), PI-SVMP+PII-SVMP (22.7 %), PIII-SVMP (15 %), CRISP (4.8), SVSP (4.6) and DIS (1.8 %) (Fig. 5A).

3.2. Shotgun proteomic profiling

To achieve a comprehensive characterization of the venom, we determined the number of toxins in representative individuals of different sizes from the five lineages of the *C. molossus* complex (*C. basiliscus* $n = 7$, *C. m. molossus* $n = 6$, *C. m. nigrescens* $n = 9$, *C. m. oaxacus* $n = 8$, and *C. ornatus* $n = 6$) using shotgun proteomics of

unfractionated venoms. Eighteen toxin families were identified across these lineages (Fig. 7, Supplementary Tables S9–S18). Notably, three-finger toxin (3FTX) and PLB were found exclusively in the venom of *C. basiliscus* individuals, whereas Kunitz peptide (KUN) was unique to *C. ornatus*. Venom factor (VF) was identified solely in the venom of *C. m. oaxacus* and *C. ornatus* individuals. Vespryn was detected in four lineages, except *C. m. molossus* (Fig. 7, Supplementary Tables S9–S18). The total number of proteins identified in each species was as follows: 56 in *C. basiliscus*, 65 in *C. m. molossus*, 75 in *C. m. nigrescens*, 78 in *C. m. oaxacus*, and 80 in *C. ornatus* (Supplementary Tables S9-S18). The number of proteins shared among all individuals within the same lineages was 39, 46, 27, 51, and 58 for *C. basiliscus*, *C. m. molossus*, *C. m. nigrescens*, *C. m. oaxacus*, and *C. ornatus*, respectively (Supplementary Tables S9–S18). CTL, SVSP, and SVMP were the protein families with the largest number of variants across the five lineages, each containing more than eight isoforms. SVSP was the protein family with the highest number of variants in *C. basiliscus* ($n = 14$), *C. m. oaxacus* ($n = 23$), and *C. ornatus* ($n = 24$). In contrast, SVMP was the toxin family containing the highest number of variants in *C. m. molossus* (19 in total: 4 PI-SVMP, 8 PII-SVMP, 7 PIII-SVMP) and *C. m. nigrescens* (21 in total: 4 PI-SVMP, 8 PII-SVMP, 9 PIII-SVMP) (Fig. 7, Supplementary Tables S9–S18). Despite the high abundance of MYO in the venom of some small snakes across four of the five lineages, no lineage exhibited more than three MYO isoforms. The range of total proteins in individual venoms within the same lineage was 38–49 for *C. basiliscus*, 51–62 for *C. m. molossus*, 43–61 for *C. m. nigrescens*, 63–70 for *C. m. oaxacus*, and 64–71 for *C. ornatus*.

In addition to qualitative analysis, we estimated the relative abundance of protein families gathered by label-free ion-intensity shotgun MS analysis. We summed the spectral intensities of proteins within the same family or subfamily as a proxy to compare their relative abundance among individual venoms across the five lineages. It is important to note that while shotgun proteomics provides a valuable approximation of the abundance of individual toxins, the quantitative use of this technique is limited due to possible intrinsic biases (for details, see references; Calvete et al., 2023; Melani et al., 2016; Weekers et al., 2024).

PLA_2, SVSP, and MYO exhibited the highest spectral intensities in the venoms of the four smallest individuals of *C. basiliscus* (CBA04, CBA05, CBA08, and CBA14). In contrast, PI-SVMP, PIII-SVMP, and SVSP were the most intense toxin families and subfamilies in the three largest individuals of *C. basiliscus* (CBA03, CBA07, and CBA16) (Fig. 2C Supplementary Tables S9 and S10). There were significant positive relationships between the intensity of PI-SVMP ($F = 35.4$, $P = 0.002$) and PIII-SVMP ($F = 27.3$; $P = 0.003$) and individual size. Conversely, there were significant negative relationships between the intensity of MYO ($F = 16.0$, $P = 0.010$), PLA_2 ($F = 51.9$, $P < 0.001$), and SVSP ($F = 19.015$, $P = 0.007$) with the size of individuals.

MYO was the toxin family with the highest spectral intensity in the smallest *C. m. molossus* individual (CMM08), whereas PIII-SVMP had the highest intensity in the remaining five *C. m. molossus* individuals (Fig. 3C, Supplementary Tables S11 and S12). There was a positive relationship between the intensity of PLA_2 ($F = 79.966$; $P < 0.001$), PI-SVMP ($F = 18.155$; $P = 0.013$), and PIII-SVMP ($F = 28.081$; $P = 0.006$) with the SVL of individuals, however, there was a significant decrease in the MYO ($F = 24.227$; $P = 0.008$) intensity and SVL.

For *C. m. nigrescens*, MYO, PIII-SVMP, and SVSP were the most intense toxin families in the venom of the six smallest individuals (CMN39, CMN40, CMN41, CMN43, CMN49, and CMN50). In contrast, PLA_2, PI-SVMP, and PIII-SVMP exhibited the highest intensities in the venom of the three largest individuals (CMN46, CMN51, and CMN52) (Fig. 4C, Supplementary Tables S13 and S14). Significant positive relationships were observed between the intensity of PI-SVMP ($F = 11.6$, $P = 0.011$), PII-SVMP ($F = 12.2$, $P = 0.010$), and PLA_2 ($F = 15.1$, $P = 0.006$) with the size of individuals, while SVSP showed a significant negative relationship with size ($F = 56.200$, $P < 0.001$).

In *C. m. oaxacus*, PIII-SVMP was the most intense toxin family in the venom of all eight individuals. PLA_2 was the second most intense toxin family in most individuals, except for CMO08, where PII-SVMP was the second most intense (Fig. 5C, Supplementary Tables S15 and S16). No

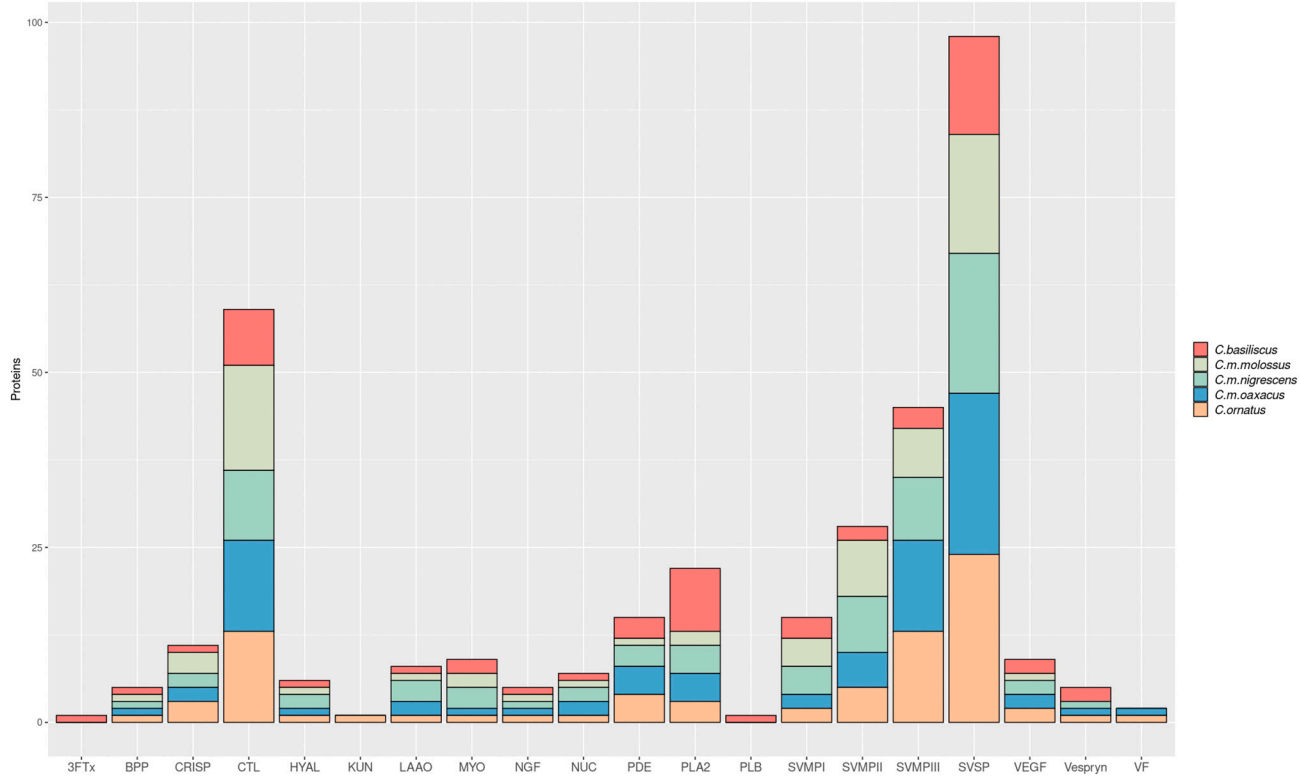

Fig. 7. Protein diversity in the five lineages within the *C. molossus* complex obtained by whole venom shotgun proteomics. Venom protein families and subfamilies identified across five lineages. Bars represent the total number of proteins identified per toxin family/subfamily in each lineage (different color).

significant relationship was found between the intensity of PLA_2, SVMP, and SVSP, and the SVL of the snakes. Nonetheless, although the PI-SVMP intensity did not significantly correlate with SVL, four (CMO03, CMO05, CMO07, and CMO09) of the five largest individuals displayed higher intensities of PI-SVMP compared to the three smallest individuals. A small amino acid sequence (TVICLPPSSDFGK) with 100 % homology with MYO was detected in the venom of all *C. m. oaxacus* individuals, but its intensity was minimal (<4,226,011) in comparison to the remaining four lineages.

In *C. ornatus*, SVSP, MYO, and PIII-SVMP were the first, second, and third most intense toxin families in the venom of the smallest individual (CO16), respectively. PLA_2, PIII-SVMP, and SVSP exhibited the highest intensities in the remaining five individuals, with variation in intensity among them (Fig. 6C, Supplementary Tables S17 and S18). PI-SVMP was also notably abundant in the two largest individuals, CO18 and CO19.

Given that acidic PLA_2, basic PLA_2, and $sPLA_2$-like can co-exist in rattlesnake venoms, we identified their presence in the venoms of individuals from the five lineages. We followed the nomenclature Dowell et al. (2016) proposed to name each PLA_2 isoform. In *C. basiliscus*, we detected two acidic PLA_2s (A1 and A2), two basic PLA_2 (B2, C2), and one $sPLA_2$-like myotoxin (K) (Supplementary Fig. S6). Among these, A2 corresponds to the acidic subunit of CTX, whereas B2 corresponds to the basic subunit of CTX. K and C2 were the least abundant isoforms in this lineage. In *C. m. molossus*, *C. m. nigrescens*, *C. m. oaxacus*, and *C. ornatus*, we identified A1 and K, which were particularly abundant in the venom of larger individuals (Supplementary Fig. S6). A basic PLA_2 (B1) was also detected in the venoms of *C. m. nigrescens* and *C. m. oaxacus*, although its presence was less significant.

3.3. Interspecific and ontogenetic variation in the protein profile of venoms in the C. molossus complex

To identify phenotypic variations associated with snake length across a larger sample of individuals from the five lineages of the *C. molossus* complex, we analyzed the venom protein profiles of 67 individuals using RP-HPLC (Supplementary Figs. S7–S11) and SDS-PAGE (Supplementary Fig. S13). We used the RP-HPLC chromatograms and the SDS-PAGE gels from representative venom proteomes as reference to estimate the relative abundance of MYO and SVMP in the remaining samples.

Peaks eluting between 30 min and 40 min predominantly contained MYO, as confirmed by the molecular mass (~5000 Da) in the venom proteomes of most lineages. The only exception was *C. m. oaxacus*, which primarily contained DIS (~7000 Da) and lacked MYO in this elution time range. The proportion of MYO in venoms varied as follows: from 0.6 % to 33.3 % ($\bar{x}$ = 13.2 %, median = 5.2 %) in *C. basiliscus*; from 1.6 % to 72 % ($\bar{x}$ = 17.6 %, median = 3.1 %) in *C. m. molossus*; from 0.5 % to 66.2 % ($\bar{x}$ = 27.6 %, median = 33.3 %) in *C. m. nigrescens*; and, from 0 % to 64.1 % ($\bar{x}$ = 7.5 %, median = 2.2 %) in *C. ornatus* (Table 2). MYO abundance decreased with age in the four lineages, as the percentage of MYO was reduced with increasing SVL (Supplementary Fig. S14 A–D). Electrophoretic profiles also confirmed that MYO (apparent mass of ~11 kDa) was more abundant in smaller individuals (SVL < 95 cm, 70 cm, 80 cm, 73 cm for *C. basiliscus*, *C. m. molossus*, *C. m. nigrescens*, and *C. ornatus*, respectively) across most lineages, except for *C. m. oaxacus* (Supplementary Fig. S13).

SVMPs were the predominant components in the fractions that eluted after 75 min in the venom chromatograms, although other toxins such as HYAL, LAAO, PDE, PLA_2, PLB, and NUC were also present. The percentage of these fractions varied among lineages: from 5.0 % to 70.3 % ($\bar{x}$ = 38.3 %, median = 48.9 %) in *C. basiliscus*; from 7.6 % to 50.2 % ($\bar{x}$ = 24.2 %, median = 19.5 %) in *C. m. molossus*; from 5.6 % to 63.1 % ($\bar{x}$ = 35.4, median = 30.6) in *C. m. nigrescens*; from 36 % to 63.3 % ($\bar{x}$ = 50.92, median = 49.5) in *C. m. oaxacus*; and from 4.7 % to 70.3 % ($\bar{x}$ = 45.5 %, median = 48.9 %) in *C. ornatus* (Table 2). The abundance of these fractions increased significantly in larger snakes across all lineages except *C. m. oaxacus* (Supplementary Fig. S14 E–I). Electrophoretic profiles of venoms revealed that the amount of PI-SVMPs and PII-SVMPs (20–25 kDa) was notably reduced in smaller snakes of the five lineages, with a marked increase in larger individuals (SVL > 95 cm, 70 cm, 80 cm, 56.5 cm, and 51.5 cm for *C. basiliscus*, *C. m. molossus*, *C. m. nigrescens*, *C. m. oaxacus*, and *C. ornatus*, respectively) (Supplementary Fig. S13).

On the other hand, CTL, CRISP, PLA_2, SVSP, and VEGF were identified in the venom fractions eluting between 41 and 75 min. However, since different toxin families tended to coelute in the same fraction in this retention time range, it was not possible to estimate the abundance of specific toxin families in this chromatogram region. Nevertheless, we estimated the percentage of SVSPs, PLA_2s, and CTL in venoms by measuring the intensity of SDS-PAGE bands with molecular masses of 11–17 kDa (PLA_2s + CTLs) and 25–48 kDa (SVSP). The electrophoretic profiles indicated that SVSPs were more abundant in smaller individuals than in larger individuals across the five lineages (Table 2, Supplementary Fig. S13). In contrast, the abundance of PLA_2s + CTLs was higher in larger individuals (SVL > 60 cm, 80 cm, 40 cm, 51.5 cm for *C. m. molossus*, *C. m. nigrescens*, *C. m. oaxacus*, and *C. ornatus*, respectively) of most lineages, except for *C. basiliscus*, where PLA_2s were more abundant in smaller snakes (SVL < 133 cm) (Table 2, Supplementary Fig. S13).

Notorious differences in the height and area of RP-HPLC fractions were also observed between juvenile and adult venom pools across the five lineages. MYO fractions (eluting at 30–40 min) were markedly more abundant (14.3–62.8 %) in juvenile venom pools compared to adult venom pools (1.1–9.8 %) in *C. basiliscus*, *C. m. molossus*, C. *m. nigrescens*, and *C. ornatus* (Table 3, Supplementary Fig. S12). Conversely, SVMPs (fractions eluting after 75 min) were more abundant in the adult venom pools (27.6–56.6 %) compared to juvenile venom pools (4.5–34.5 %) across the five lineages (Table 3, Supplementary Fig. S12).

3.4. Proteolytic activity of individual venoms

We assessed the proteolytic activity of the venoms from 58 individuals across the five lineages (*C. basiliscus* $n = 13$, *C. m. molossus* $n = 6$, *C. m. nigrescens* $n = 13$, *C. m. oaxacus* $n = 10$, and *C. ornatus* $n = 16$) (Table 2). The proteolytic activity ranged from 0.08 to 8.75 U/mg ($\bar{x}$: 3.64 ± 3.31 U/mg) for *C. basiliscus*; 0.29 to 6.40 U/mg ($\bar{x}$: 3.83 ± 2.20 U/mg) for *C. m. molossus*; 0.47 to 8.67 U/mg ($\bar{x}$: 3.51 ± 2.53 U/mg) for *C. m. nigrescens*; 0.83 to 6.16 U/mg ($\bar{x}$: 4.14 ± 1.70 U/mg) for *C. m. oaxacus*; and 0.66 to 7.26 U/mg ($\bar{x}$: 5.50 ± 2.02 U/mg) for *C. ornatus* (Supplementary Fig. S15A). There was no significant difference in the proteolytic activity among the five lineages. However, a significant positive relationship ($R2 = 0.896$, $P < 001$; $R2 = 0.891$, $P = 0.005$; $R2 = 0.663$, $P < 0.001$; $R2 = 0.725$, $P = 0.002$; and $R2 = 0.253$, $P = 0.047$ for *C. basiliscus*, *C. m. molossus*, *C. m. nigrescens*, *C. m. oaxacus*, and *C. ornatus*, respectively) was observed between the SVL and proteolytic activity in the venoms of the five lineages (Supplementary Fig. S14 J–N).

3.5. Phospholipase A_2 (PLA_2) activity of individual venoms

We measured the PLA_2 activity of venom from 38 individuals across the five lineages (*C. basiliscus* $n = 13$, *C. m. molossus* $n = 6$, *C. m. nigrescens* $n = 6$, *C. m. oaxacus* $n = 7$, and *C. ornatus* $n = 6$) (Table 2). PLA_2 activity was significantly ($P < 0.05$) higher in *C. basiliscus* venoms ($\bar{x}$: 4.68 ± 1.55 Δ405 nm) compared to *C. m. oaxacus* ($\bar{x}$: 1.21 ± 0.46 Δ405 nm) and *C. ornatus* ($\bar{x}$: 1.48 ± 0.60 Δ405 nm) venoms (Supplementary Fig. S15B). Additionally, a significant negative relationship ($R2 = 0.486$; $P = 0.008$) was found between SVL and PLA_2 activity in *C. basiliscus* (Supplementary Fig. S14O). In contrast, a significant positive relationship ($R2 = 0.885$; $P = 0.005$) was observed between the SVL and PLA_2 activity in *C. m. nigrescens* (Supplementary Fig. S14Q).

3.6. Fibrinogenolytic activity

We evaluated the fibrinogenolytic activity of venom from six representative individuals of each lineage. The venom from six *C. basiliscus* individuals completely cleaved both α and β subunits of fibrinogen. However, only the two smallest individuals (CBA05 and CBA15) exhibited fibrinogen clotting (Supplementary Fig. S16A). *C. m. molossus* venoms displayed a partial degradation of α and β subunits of fibrinogen (Supplementary Fig. S16B), with only the three smallest individuals (CMM07, CMM08, and CMM09) forming fibrin clots (Supplementary Fig. S16B). The venom of the six *C. m. nigrescens* cleaved the α subunit of fibrinogen, but only the four largest individuals (CMN41, CMN46, CMN51, CMN52) also cleaved the β subunit (Supplementary Fig. S16C). For this species, the venom of the three smallest individuals (CMN39, CMN40, and CMN41) formed a fibrin clot before being loaded into SDS-PAGE gels. The venom of the six *C. m. oaxacus* partially

Table 2
Biological activities and abundance of MYO, SVMP, PLA_2 + CTL, and SVSP in individual venoms.

Venom	i.v. LD_{50} (μg/g)	Proteolytic activity (U/mg)	PLA_2 activity (ΔAbs 405 nm)	%MYO	%SVMPs	%PLA_2 + CTL	%SVSP
CBA15	ND	0.41 ± 0.08	4.86	ND	ND	32	15.5
CBA14	ND	0.50 ± 0.12	6.20	ND	ND	21.7	9.0
CBA05	ND	0.133 ± 0.02	5.97	26.6	7.1	44.2	7.3
CBA06	0.76 (0.74–0.78)	ND	ND	33.3	5.0	29.7	11
CBA08	ND	0.33 ± 0.15	6.17	ND	ND	ND	ND
CBA04	0.18 (0.16–0.20)	0.075 ± 0.01	5.97	27.8	6.6	52.1	11.8
CBA09	ND	0.48 ± 0.13	6.14	ND	ND	25.9	18.1
CBA12	ND	5.50 ± 0.07	3.55	ND	ND	6.5	16.8
CBA11	ND	8.75 ± 0.37	3.93	0.6	60.7	6.8	18
CBA10	ND	7.06 ± 0.22	3.0	3.1	70.3	9.2	15.4
CBA07	3.36 (3.30–3.41)	6.71 ± 0.30	4.33	5.6	58.9	12.3	14.7
CBA16	ND	5.93 ± 0.58	1.23	ND	ND	ND	ND
CBA13	ND	5.10 ± 0.18	3.68	3.8	44.7	11.04	15.4
CBA03	1.95 (1.52–2.30)	6.44 ± 0.24	5.86	4.8	53.1	17.4	17.6
CMM08	1.53 (1.51–1.55)	0.29 ± 0.02	2.07	72.0	7.6	9.0	36.3
CMM09	ND	3.39 ± 0.21	3.73	43.7	8.4	9.5	30.3
CMM07	ND	3.4 ± 0.12	4.39	19.6	19.5	26.8	17.7
CMM05	2.75 (2.66–2.85)	3.53 ± 0.20	3.91	2.3	35.4	38.8	11.38
CMM04	1.00 (0.97–1.03)	6.4 ± 0.27	2.65	1.9	50.2	36.07	6.0
CMM06	1.82 (1.70–1.99)	6.0 ± 0.23	3.05	1.6	43.4	47	8.9
CMN49	ND	1.12 ± 0.08	ND	54.3	5.6	ND	ND
CMN50	ND	0.47 ± 0.09	ND	50.5	20.1	ND	ND
CMN44	ND	2.64 ± 0.12	ND	45.2	14.3	4.7	38.5
CMN43	ND	0.47 ± 0.04	ND	45.1	13.2	9.5	25.8
CMN40	0.72 (0.69–0.76)	0.81 ± 0.02	1.41	66.2	9.6	0.8	19.5
CMN39	ND	2.31 ± 0.07	1.03	38.6	19.1	6.3	37.9
CMN41	1.03 (0.87–1.24)	4.053 ± 0.14	1.44	28.1	32.0	6.2	26.2
CMN31	ND	3.13 ± 0.09	ND	42.9	29.2	0.7	23.7
CMN51	3.02 (2.68–3.43)	5.93 ± 0.13	2.11	0.6	59.0	ND	ND
CMN06	ND	5.18 ± 0.17	ND	1.3	56.7	46.2	1.5
CMN52	ND	8.67 ± 0.59	2.100	0.5	62.00	ND	ND
CMN46	7.49 (7.07–7.88)	5.33 ± 0.15	2.400	0.7	55.1	48.5	2.0
CMN42	ND	5.581 ± 0.11	ND	2.7	63.1	39.5	0.6
CMO10	0.10 (0.08–0.11)	0.83 ± 0.00	ND	0	36.2	ND	ND
CMO08	0.27 (0.24–0.30)	3.43 ± 0.10	0.75	0	36.0	1.88	23.5
CMO02	ND	2.76 ± 0.21	0.62	0	48.7	1.33	19.8
CMO130	ND	3.19 ± 0.07	1.84	ND	ND	19.5	35.4
CMO11	2.36 (2.23–2.50)	3.47 ± 0.09	1.08	0	48.5	19.7	27.04
CMO09	3.78 (3.34–4.20)	5.4 ± 0.1	1.63	0	59.7	18.0	18.0
CMO06	3.89 (3.50–4.3)	4.71 ± 0.14	ND	0	62.3	ND	ND
CMO07	2.37 (2.09–2.59)	5.33 ± 0.17	1.42	0	49.5	20.0	7.9
CMO03	3.75 (3.26–4.24)	6.16 ± 0.21	1.15	0	47.8	34.6	8.7
CMO05	5.87 (5.67–6.07)	6.12 ± 0.18	ND	0	54.0	ND	ND
CO16	2.07 (1.66–2.65)	0.66 ± 0.00	0.51	64.1	4.7	9.5	20.4
CO10	1.83 (1.48–2.09)	5.6 ± 0.15	1.75	13.6	27.8	32.4	16.6
CO15	ND	5.84 ± 0.13	1.07	16.8	49.1	36.8	2.1
CO09	3.65 (3.26–3.95)	6.55 ± 0.20	ND	0.7	50	35.1	7.6
CO08	3.17 (3.16–3.17)	1.58 ± 0.06	1.83	1.3	40.4	49.3	1.4
CO07	ND	6.46 ± 0.26	ND	2.0	42.6	38.6	3.1
CO04	ND	6.58 ± 0.13	ND	0.6	52.1	52.2	4.3
CO13	1.96 (1.86–2.06)	3.28 ± 0.08	2.19	3.2	35.8	46.2	11.6
CO19	3.54 (3.04–4.05)	7.1 ± 0.22	ND	0.8	70.3	ND	ND
CO14	ND	6.21 ± 0.15	ND	3.8	37.9	39.3	17.1
CO18	3.74 (2.86–4.62)	7.19 ± 0.21	1.52	2.5	54.3	ND	ND
CO12	ND	6.2 ± 0.13	ND	5.8	48.6	49.5	1.8
CO06	ND	7.12 ± 0.23	ND	3.8	55.1	34.2	2.2
CO05	ND	4.18 ± 0.18	ND	1.3	58.9	23.1	1.7
CO03	ND	6.27 ± 0.23	ND	0	46.6	33.0	1.0
CO11	3.17 (3.17–3.17)	7.26 ± 0.19	ND	0	53.4	28.9	5.3

%MYO: Percent of MYO in venoms estimated from the area under the curve of fractions eluting from 30 to 40 min. %SVMP: Percent of SVMPs in venoms estimated from the area under the curve of fractions eluting after 75 min. %PLA_2 + CTL and %SVSP: Percent of PLA_2s + CTL and SVSPs in venoms estimated by densitometry from SDS-PAGE bands with a molecular mass in the range of 11 kDa–17 kDa and 25 kDa–48 kDa, respectively. ND: not determined due to lack of venom. Snakes were sorted by SVL from smallest to largest.

degraded both α and β subunits of fibrinogen, but only the three smallest individuals (CMO08, CMO11, CMO130) exhibited fibrinogen clotting (Supplementary Fig. S16D). Finally, while all *C. ornatus* venoms demonstrated proteolytic activity against both α and β chains of fibrinogen, the extent of degradation varied among individuals (Supplementary Fig. S16E). The three venoms that induced fibrin clots were CO08, CO13, and CO16.

When we preincubated venoms with EDTA (a zinc-chelating agent) or PMSF (an SVSP inhibitor), we observed only partial inhibition of fibrinogenolytic activity. In contrast, simultaneous preincubation with both EDTA and PMSF resulted in complete abolition of fibrinogenolytic activity. These results indicate that both SVMPs and SVSPs contribute to fibrinogenolytic activity, though their influence varies among lineages and age classes.

3.7. Lethality of individual and pooled venoms

We assessed the i.v. LD_{50} of the venoms from 28 individuals across the five lineages (*C. basiliscus* $n = 4$, *C. m. molossus* $n = 4$, *C. m. nigrescens* $n = 4$, *C. m. oaxacus* $n = 8$, and *C. ornatus* $n = 8$) in mice (Table 2). The range of i.v. LD_{50} values for each lineage was as follows: *C. basiliscus*, 0.18 μg/g–3.36 μg/g ($\bar{x}$:1.56 ± 1.4 μg/g), *C. m. molossus*, 1.00 μg/g–2.75 μg/g ($\bar{x}$: 1.77 ± 0.7 μg/g); *C. m. nigrescens*, 0.72 μg/g–7.49 μg/g ($\bar{x}$: 3.06 ± 3.1 μg/g); *C. m. oaxacus*, 0.10 μg/g–5.87 μg/g ($\bar{x}$: 2.80 ± 2.0 μg/g), and *C. ornatus*, 1.82 μg/g–3.74 μg/g ($\bar{x}$: 2.89 ± 0.8 μg/g) (Supplementary Fig. S15C). There were no significant differences in the lethality among the five lineages ($P = 0.572$). However, the five individuals (CBA04, CBA06, CMN40, CMO08, and CMO10) with an i.v. LD_{50} of <1 μg/g (most lethal) had an SVL of <60 cm (Table 1), indicating that the venom of smaller snakes tends to be more lethal to mice than the venom of larger snakes in *C. basiliscus*, *C. m. nigrescens*, and *C. m. oaxacus*.

Intravenous LD_{50} assays with pooled venoms also confirmed that for *C. basiliscus*, *C. m. nigrescens* and C. *oaxacus*, the venom from smaller individuals is approximately 17.5, 2.0, and 6.4-fold more lethal than the venom from larger individuals, respectively (Table 3). In contrast, pooled venoms from small and large individuals of *C. m. molossus* and *C. ornatus* displayed similar LD_{50} values.

3.8. Lethality of individual venoms toward different biological models

The MYO-rich venom of the small *C. m. nigrescens* individual (CMN40) was lethal (i.p. LD_{50}: 3.4 μg/g (3.4–3.5 μg/g)) only to the mammal model (mouse), as no mortality was recorded injecting up to 100 μg/g body weight of venom to the reptile model (black iguana). Additionally, the tetanic effect in hind limbs produced by MYO was observed only in mice. The SVMP-rich venoms of the large individuals of *C. m. nigrescens* (CMN46) and *C. m. oaxacus* (CMO03) were also several times more lethal to the mice (i.p. LD_{50}: 9.8 μg/g (9.1 μg/g–10.2 μg/g) and i.p. LD_{50}: 6.9 μg/g (6.8 μg/g–6.9 μg/g), respectively) than to black iguanas (i.p. LD_{50}: 89.5 μg/g (89.4 μg/g–89.5 μg/g) and i.p. LD_{50}: 62.2 μg/g (45.5 μg/g–84.2 μg/g), respectively).

3.9. Partial isolation of lethal components in the CMO08 venom

Given that the venom of individual CMO08 was highly lethal to mice (i.v. LD_{50} 0.27 μg/g) despite lacking CTX homologs or MYO, we investigated the identity of the lethal component(s) present in this venom. We fractionated the CMO08 venom using gel filtration on a Sephadex G-75 column and assessed the lethality of fractions in mice. Four fractions were obtained (Supplementary Fig. S17A), but only Fraction 1 (F1) was lethal when injected i.v. at 25 μg/mouse (3/3 deaths). The final i.v. LD_{50} of F1 was 0.74 μg/g (0.64–0.83 μg/g). F1 was further separated using SDS-PAGE (Supplementary Fig. S17B) and RP-HPLC (Supplementary Fig. S17D). Most proteins in F1 eluted after 70 min in RP-HPLC (Supplementary Fig. S17D) and the most intense bands in SDS-PAGE had molecular masses ranging between 48 and 75 kDa (Supplementary Fig. S17B). These results suggest that the lethal components in CMO08 venom likely belong to the PIII-SVMP protein family.

3.10. Immunorecognition of whole venoms by Antivipmyn®

We evaluated the immunological binding capability of Antivipmyn® against venom pools from both juvenile and adult individuals of the five

Table 3
MYO and SVMP abundance with LD_{50}, EC_{50}, and ED_{50} values in adult and juvenile venom pools from the five lineages in the *C. molossus* complex.

Adult venom pools	% MYO	% SVMP	i.v. LD_{50} (μg/g)	Antivipmyn EC_{50} (μg/mL)	ED_{50} (μL AV/$3LD_{50}$)	ED_{50} (mgAV/mgV)
C. basiliscus (CBA03 and CBA07)	9.8	50	3.31 (3.27–3.35)	5.8 (4.6–7.2)	205.7 (201.2–209.8)	6.7
C. m. molossus (CMM01, CMM02, CMM03, CMM04, CMM05, and CMM06).	3.7	27.6	0.82 (0.82–0.83)	4.3 (3.6–5.2)	60.1 (55.7–65.4)	7.7
C. m. nigrescens (CMN42, CMN46, CMN51, and CMN52).	1.1	53.5	4.85 (4.8–4.9)	4.7 (3.5–6.5)	85.1 (83.07–87.36)	1.9
C. m. oaxacus (CMO03, CMO05, CMO06, CMO07, and CMO09).	0	56.6	5.77 (5.04–6.3)	5.2 (4.1–6.8)	194.9 (191.2–198.6)	3.6
C. ornatus (CO06, CO07, CO08, CO12, CO13, CO14, CO18, and CO25).	3.0	46.6	2.6 (2.6–2.6)	22.7 (17.7–30.9)	21.7 (21.75–21.75)	0.9

Juvenile venom pools	% MYO	% SVMP	i.v. LD_{50} (μg/g)	Antivipmyn EC_{50} (μg/mL)	ED_{50} (μL AV/$3LD_{50}$)	ED_{50} (mgAV/mgV)
C. basiliscus (CBA04, CBA05, and CBA06).	28.4	4.5	0.19 (0.19–0.20)	52.7 (24–477)*	19.1 (18.15–19.97)	10.5
C. m. molossus (CMM07, CMM08, and CMM09).	34.0	14.8	1.01 (0.80–1.27)	6.6 (5.4–8.2)	74.6 (71.0–78.41)	8.0
C. m. nigrescens (CMN31, CMN39, CMN40, CMN41, CMN43, and CMN44).	62.8	9.2	2.35 (2.10–2.63)	2.7 (2.0–3.5)	309.0 (266.5–349.7)	14.1
C. m. oaxacus (CMO01, CMO02, CMO04, CMO08, CMO10, and CMO11).	0	34.2	0.90 (0.73–1.07)	3.06 (2.4–3.8)	24.9 (20.82–31.75)	3.0
C. ornatus (CO10, CO15, and CO16).	14.3	34.5	3.0 (2.5–3.5)	ND	18.6 (17.7–19.6)	0.7

Individual venoms forming each pool are shown. Antivipmyn® immurecognition against juvenile and adult pooled venoms of five lineages in the *C. molossus* complex expressed in EC_{50} (μg/mL). *The final EC_{50} was not determined since the titration curves do not reach a clear plateau. ED_{50}: Median Effective Dose, the dose of antivenom that induces survival in 50 % of intravenous (i.v.) injected mice (18–20 g) with 3 × LD_{50} of each venom. μL AV/$3LD_{50}$: microliters of antivenom that neutralized 3 × LD_{50}. mgAV/mgV: milligrams of antivenom that neutralized 1 mg of venom. ND: not determined due to insufficient venom.

lineages from the *C. molossus* complex using ELISA (Table 3). The venom of juvenile *C. basiliscus* was not fully recognized by Antivipmyn® at the concentrations tested, since the titration curve did not reach a clear plateau; therefore, its titer is considered unreliable (Supplementary Fig. S18).

For adult and juvenile *C. m. molossus*, *C. m. nigrescens* and C. *m. oaxacus*, similar venom-binding titers of Antivipmyn® were obtained. Due to the limited amount of venom pool available from juvenile *C. ornatus*, we could only determine the EC_{50} value of venom from the adults, which was the least recognized among the adult venoms (Table 3).

3.11. Neutralization of lethal activity of venom pools

Variation was observed in the neutralization capacity of Antivipmyn® against juvenile and adult venom pools of the five lineages from the *C. molossus* complex (Table 3). Interestingly, the results varied depending on how the median effective dose (ED_{50}) was expressed.

When ED_{50} was expressed as microliters of antivenom required to neutralize three LD_{50} (μL AV/3LD_{50}), the venom pools needing the most antivenom were those from juvenile *C. m. nigrescens* and adult *C. basiliscus* and *C. m. oaxacus* (309, 205.7, and 194.9 μL AV/3LD_{50}, respectively). In contrast, the venom pools requiring fewer microliters of antivenom were from juvenile *C. basiliscus*, *C. m. oaxacus* and *C. ornatus*, and adult *C. ornatus* (19.1, 24.9, 18.6, and 21.7 μL AV/3LD_{50}, respectively).

When ED_{50} was expressed as milligrams of antivenom required to neutralize 1 mg of venom (mg AV/mg V), juvenile *C. basiliscus* and *C. m. nigrescens* needed more milligrams of antivenom to neutralize 1 mg of venom (10.5 and 14.1 mg AV/mg V, respectively). Conversely, the venom pools that required fewer milligrams of antivenom to neutralize 1 mg of venom were from juvenile and adult *C. ornatus* (0.7 and 0.9 mg AV/mg V, respectively).

4. Discussion

4.1. Venom variation among and within lineages

Using two proteomic approaches, we have comprehensively characterized the venom composition of five rattlesnake lineages classified within the *C. molossus* complex. Our analysis identified at least eighteen toxin families across these lineages, with varying numbers of isoforms detected both within and among lineages (Figs. 2–7). For instance, within the PLA_2 family, CTX was exclusively found in *C. basiliscus* (Fig. 2). Our study also delineated the ontogenetic patterns in venom composition within each lineage. In general, smaller specimens of *C. basiliscus* (SVL < 55 cm) exhibited venom rich in MYO, SVSP, and PLA_2 (including CTX), whereas the venoms of larger individuals (SVL > 130 cm) were dominated by SVMP (particularly PI- and PIII-SVMPs) (Fig. 2). In *C. m. molossus*, *C. m. nigrescens*, and *C. ornatus*, there was a transition from venoms rich in MYO, PIII-SVMP, and SVSP in smaller individuals to venoms rich in PLA_2 and PI-SVMP as the snakes grew larger (Figs. 3, 4, and 6). In *C. m. oaxacus*, both small and large individuals had PIII-SVMP-rich venoms; however, smaller individuals tended to have more SVSP, while larger individuals tended to have more PI-SVMP and PLA_2 (Fig. 5). Interestingly, this was the only lineage where MYOs were absent in juvenile venom. These trends were further supported by RP-HPLC chromatograms and electrophoretic profiles (Supplementary Figs. S7–S13).

It is noteworthy that our sampling of *C. basiliscus* (SVL: 39–157 cm), *C. m. nigrescens* (SVL: 28–88 cm), and *C. m. oaxacus* (SVL: 36.9–99 cm) encompassed nearly the entire size range for these lineages, ensuring venom samples from both juveniles and adults. For *C. ornatus*, the SVL ranged from 45.5 cm to 95 cm, suggesting that adults were well represented. Unfortunately, for *C. m. molossus*, the size range of the six individuals collected was narrow (SVL: 49.5–75 cm), and there is a possibility that individuals smaller or larger than those sampled here may have different venom compositions.

In snakes of the same lineage but distinct sizes, variations in venom toxin number and abundance likely result from the transcriptional (e.g., via cis-regulatory elements and trans-regulatory factors, and epigenomic modifications) and translational regulation (e.g., via microRNAs) of venom genes, and posttranslational modifications of proteins (Durban et al., 2017, 2013; Gopalan et al., 2024; Hogan et al., 2024; Margres et al., 2021a; Westfall et al., 2023). In snakes of different lineages (and potentially within the same lineage), venom composition may also be influenced by variation in the number of venom genes, in addition to these regulatory processes. Genomic studies in pit vipers have revealed variations in the number of genes encoding for toxin families such as MYO, PLA_2, SVMP, and SVSP due to gene gain or loss processes (Dantas Almeida et al., 2021; Dowell et al., 2018, 2016; Giorgianni et al., 2020; Margres et al., 2021a, 2017; Schield et al., 2019). Therefore, further investigation is needed to elucidate the molecular mechanisms underlying inter- and intraspecific venom variation within the *C. molossus* complex.

4.2. Association between venom composition and biological activities

In rattlesnakes, dietary shifts over their lifetime have been proposed as critical drivers of ontogenetic changes in venom composition (Hogan et al., 2024; Mackessy, 2010a; Mackessy et al., 2003; Schonour et al., 2020). For instance, *Crotalus concolor* undergoes ontogenetic shifts in its diet, transitioning from a juvenile diet primarily consisting of ectothermic animals (e.g., lizards) to an adult diet that mainly includes endothermal animals (e.g., mammals). Alongside this dietary shift, the venom of *C. concolor* showed an increased abundance of MYO in adults (Mackessy et al., 2003). Interestingly, MYO has been suggested to be a toxin that may specifically target mammals, as it induces rapid tetanic paralysis in mice but shows no apparent effect on certain lizard genera like *Sceloporus*, *Hemidactylus*, and *Anolis* (Mackessy and Saviola, 2016; Smith et al., 2023). The prevalence of MYO in the venom of northern *C. viridis* populations, which primarily consume mammals, compared to the prevalence of SVMP in the venom of southern *C. viridis* populations with a more diverse prey diet, supports this hypothesis (Smith et al., 2023). In addition, the MYO-rich venom of *C. viridis* was approximately 30 times more lethal to a population of Ord's Kangaroo Rat (*Dipodomys ordii*) where *C. viridis* with a venom rich in SVMP is distributed than to a co-occurring population of *D. ordii* (Balchan et al., 2024). Our results support the specificity of MYO toward mammals. Specifically, the MYO-rich venom from a juvenile *C. m. nigrescens* was more lethal to mice than the SVMP-rich venom from both adult *C. m. nigrescens* and *C. m. oaxacus*; however, it did not cause death or induce hind limb paralysis in black iguanas, even when administered in considerably large quantities. Therefore, the prominent presence of MYO in the venom of juvenile individuals from *C. basiliscus*, *C. m. molossus*, *C. m. nigrescens*, and *C. ornatus* could confer a trophic advantage during this stage of life. A recent study (Carbajal-Márquez et al., 2023) indicated that *C. basiliscus*, *C. m. nigrescens*, and *C. m. oaxacus* predominantly feed on mammals in all their life stages, although other biological groups such as lizards and birds have also been reported in the diet of various lineages within the *C. molossus* complex (Balderas-Valdivia et al., 2009; Funk, 1964; Holding et al., 2021; Klauber, 1972). A comprehensive study of the diet of all lineages within the *C. molossus* complex across different geographic regions and age classes is needed to ascertain whether interspecific and ontogenetic variation in MYO levels correlate with dietary differences.

Acidic PLA_2 (A1) and $sPLA_2$-like myotoxins (K) were detected in the venom of *C. m. molossus*, *C. m. nigrescens*, *C. m. oaxacus*, and *C. ornatus*, being particularly abundant in larger individuals from these lineages (Supplementary Fig. S6). Basic PLA_2 (B1) was also found in the venom of *C. m. nigrescens* and *C. m. oaxacus* individuals, although in minor proportions (Supplementary Fig. S6). Basic PLA_2s and $sPLA_2$-like myotoxins generally exhibit higher myotoxic effects compared to acidic PLA_2s

(Bonfim et al., 2001; Fernández et al., 2010; Jiménez-Charris et al., 2016; Lomonte, 2023). While both acidic and basic PLA_2s share similar enzymatic activities, $sPLA_2$-like myotoxins lack catalytic activity (Fernández et al., 2010). Moreover, acidic PLA_2s and $sPLA_2$-like myotoxins are less lethal to mice than basic PLA_2s (Jiménez-Charris et al., 2016; Lomonte, 2023; Lomonte et al., 2009; Van der Laat et al., 2013), and it has been proposed that the acidic PLA_2s might have digestive roles. Synergism between basic PLA_2s and $sPLA_2$-like myotoxins and between acidic and basic PLA_2s has been reported, where the former enhances the cytotoxic and myotoxic effects of the latter (Jiménez-Charris et al., 2016; Mora-Obando et al., 2014). Therefore, synergistic actions among different PLA_2 isoforms are likely to contribute to increased myotoxicity and lethality of the venom of adult *C. m. molossus*, *C. m. nigrescens*, *C. m. oaxacus*, and *C. ornatus*. On the other hand, *C. basiliscus* was the only lineage whose venom contained two acidic PLA_2 (A1, A2), one basic PLA_2 (B2), and K (Supplementary Fig. S6). Given the catalytic activity of A1, A2, and B2, the significantly higher phospholipase A_2 activity in this species' venom (Supplementary Fig. S14) is likely due to the combined actions of these three PLA_2 isoforms.

A consistent finding across all five lineages of the *C. molossus* complex was the high abundance of SVMPs in larger individuals, constituting over 50 % of venom composition in some cases (Figs. 2–6, Tables 2 and 3). However, while PII- and PIII-SVMP were present in relatively similar proportions in the venom of all age classes across the five lineages, PI-SVMPs were particularly abundant in larger snakes (Figs. 2–6). A similar ontogenetic shift from low- to high-PI-SVMP venom phenotypes has been observed in several *Bothrops* species (Alape-Girón et al., 2008; Guércio et al., 2006; Mora-Obando et al., 2020; Núñez et al., 2009; Zelanis et al., 2010). PI-SVMPs contain a single metalloproteinase domain responsible for activities such as hemorrhage, inflammation, fibrinogenolysis, fibrinolysis, and apoptosis. In contrast, PII and PIII-SVMPs possess additional domains (disintegrin, disintegrin/like, and cysteine-rich), which contribute to effects such as platelet aggregation inhibition, cell adhesion inhibition, and enhanced metalloproteinase activity (Tosin et al., 2020). It has been postulated that the presence of additional domains in PII-SVMP and PIII-SVMP enables them to target microvessels, which makes them more hemorrhagic than PI-SVMP (Gutiérrez et al., 2016). Despite their varied biological activities, all three SVMP subclasses can hydrolyze casein/azocasein (Macedo and Fox, 2016) due to their common metalloproteinase domain. Accordingly, the SVMP-rich venoms of larger individuals of the five lineages in the *C. molossus* complex were more proteolytic than the venom of smaller individuals containing low amounts of SVMPs (particularly PI-SVMPs) (Supplementary Fig. S15). Thereby, the presence of diverse SVMP subclasses in larger individuals' venom likely aids in subjugating and digestion of larger, heavier prey (Gutierrez et al., 2009).

SVSPs are proteolytic enzymes with molecular masses ranging from 26 kDa to 67 kDa, and their action causes an imbalance in the prey hemostatic system (Serrano, 2013; Serrano and Maroun, 2005). Particularly, snake venom thrombin-like enzymes (SVTLEs), a subset of SVSPs, exhibit thrombin-like activity without being identical to thrombin. Unlike thrombin, which cleaves fibrinogen's α- and β-chains to form stable fibrin clots, SVTLEs may cleave both chains of fibrinogen (though with higher affinity for one) or only one of them, producing unstable fibrin clots (Mackessy, 2010b; Ullah et al., 2018). While the inability to activate factor XIII may contribute to fibrin clot instability, substantial evidence indicates that SVTLEs directly act on fibrinogen to produce abnormal fibrin clots. These clots are significantly weaker at this stage compared to those formed by thrombin, even in the absence of factor XIII (Debono et al., 2019b, 2019a; Youngman et al., 2019). In contrast, most SVMPs, especially P-I SVMPs, selectively cleave the fibrinogen α-chain, although some can cleave other chains as well (Sanchez et al., 2017). However, SVMPs are less specific in the manner that they hydrolyze fibrinogen than SVTLE (Mackessy, 2010b), and they do not generate transient fibrin clots but dissolve them (Sanchez et al., 2017). We observed inter- and intraspecific variations in fibrinogen cleavage patterns among individuals from the *C. molossus* complex (Supplementary Fig. S16). More specifically, venoms differed in their affinity toward α- and β-chains of fibrinogen. In addition, preincubation of venoms with EDTA (an SVMP-inhibitor) and PMSF (an SVSP-inhibitor) generated different patterns of partial inhibition of fibrinogen hydrolysis. Only the simultaneous preincubation of both inhibitors with venoms completely abolished the fibrinogenolytic activity, indicating that both SVMPs and SVSPs play a role in this activity (Supplementary Fig. S16). Our results suggest that both SVMPs and SVSPs are responsible for the fibrinogenolytic activity in venoms of the five lineages from the *C. molossus* complex; however, different proportions of fibrinogenolytic SVMPs and SVSPs are found in venoms of the five lineages and individuals with different SVL. For instance, five venoms (CBA04, CMM08, CMN41, CMO08, CO16) that clotted fibrinogen had higher percentages of SVSPs than PI-SVMPs (Figs. 2–6, Supplementary Figs. S7–S13). These results suggest that although most venoms likely contain SVTLEs, their thrombin-like activity may only be detected in the test when the fibrinogenolytic-SVMPs competing for the same substrate are not present or are present in insignificant amounts. Supporting the above, Meléndez-Martínez et al. (2020) reported that inhibition of SVMPs in venoms of some rattlesnakes including *C. m. nigrescens* and *C. ornatus* allowed SVSPs to clot fibrinogen.

In *C. basiliscus*, *C. m. nigrescens*, and *C. oaxacus*, the venom of smaller individuals was more lethal to mice than larger individuals (Tables 2 and 3). The pattern may reflect prey-driven selection, with venom adjusting to target prey species as the snakes grow (Andrade and Abe, 1999). However, further evidence is required to confirm this relationship. Different toxin families are likely responsible for this increased lethality across these three lineages. In *C. basiliscus*, the higher abundance of CTX in the venom of smaller individuals likely contributed to their increased lethality, as previously reported for this species (Colis-Torres et al., 2022). For *C. m. nigrescens*, juvenile venoms containing high proportions of MYO, SVSP, and PIII-SVMPs (e.g. CMN40 and CMN41) were more lethal than adult venoms with lower amounts of these toxin families (e.g. CMN46). Therefore, the combined action between these three toxin families is likely responsible for the higher lethality observed in smaller snakes in this lineage. In *C. m. oaxacus*, which lacks CTX and has minimal MYO, our partial purification of the lethal components from the venom of a small individual (CMO08) indicates that PIII-SVMPs are the main contributors to higher lethality in juveniles (Supplementary Fig. S12). However, PIII-SVMPs were also abundant in the venom of larger *C. m. oaxacus* individuals. Thereby, the distinct lethality between small and large individuals in *C. m. oaxacus* may be attributed to the difference in the abundance of other toxin families. For instance, SVSPs were more abundant in smaller snakes, and PLA_2s, PI-SVMPs, and PII-SVMPs were more prevalent in larger snakes. Another possibility is that specific more lethal-PIII-SVMP isoform(s) are present only or mostly in juvenile *C. m. oaxacus* venoms. However, we could not detect a pattern that indicates that.

Although the LD_{50} values were relatively similar among individuals of different sizes in *C. m. molossus* and *C. ornatus*, we cannot exclude the possibility that individuals outside the size range evaluated in our study may exhibit differences in their lethality, as these two lineages were precisely the ones with the shortest size range sampled.

4.3. Implications of venom variation in snakebites and antivenom treatment

The four most abundant toxin families in the venom of individuals from the five lineages of the *C. molossus* complex -PLA_2, MYO, SVMP, SVSP- are also considered the most toxic to humans. The remaining toxin families are considered to play a less important role in venom toxicity (Gutiérrez et al., 2021a). In that sense, the variation in the abundance of these four toxin families, both among and within lineages, may be

reflected in the clinical manifestations observed in envenoming. For instance, bites by viperids with venoms rich in myotoxic PLA_2s, SVMPs, and SVSPs typically induce effects such as edema, myonecrosis, local and systemic hemorrhage, and coagulopathy (Gutiérrez et al., 2017a). Conversely, an envenomation by a midget-faded rattlesnake (*Crotalus oreganus concolor*), with a venom rich in MYO (60 %) and neurotoxic PLA_2s (15 %) but low in SVMPs (1 %) elicited generalized paresthesia, blurred vision, and waves of spastic, tetany-like symptoms of the hands and feet. However, no bleeding was observed at any moment (Keyler et al., 2020). Given their wide distribution in Mexico and defensive behavior, lineages of the *C. molossus* complex are likely responsible for many snakebites in this country (Neri-Castro et al., 2020), however, the species involved in most cases are most often not documented. The only three reports in the literature of envenomation by the Northern Blacktail Rattlesnake (*C. m. molossus*) described moderate to mild pathophysiological alterations with symptoms including pain, edema, ecchymosis, coagulopathy, thrombocytopenia, and hemorrhagic blebs. Two of the cases likely involved adult snakes (84 cm and 91 cm long), while the third case probably involved a juvenile snake (53 cm long) (Hardy et al., 1982; Yarema and Curry, 2005). Envenomation by an adult *C. basiliscus* resulted in shock, ventricular arrhythmia, coagulopathy, and compartment syndrome, suggesting a severe envenomation (Meyer et al., 2017).

Guadarrama-Martínez et al. (2024) classified the neutralization potency of Antivipmyn® toward venoms of nine viperid species as follows: well (1.0–8.9 mgAV/mgV), medium (9–16.9 mgAV/mgV), poorly (17–24.9 mgAV/mgV), and very poorly (25 mgAV/mgV). According to this classification, eight venom pools (adults of the five lineages and juveniles *C. m. molossus*, *C. m. oaxacus*, *C. ornatus*) were well-neutralized. In comparison, two venom pools (*C. basiliscus* and *C. m. nigrescens* juveniles) were medium-neutralized (Table 3). Previously, Sánchez et al. (2003) reported that among 15 snake venoms from various pit viper species, only the pooled venom of four *C. m. molossus* individuals were not neutralized by CroFab antivenom, one of the antivenoms available in the United States. Conversely, Antivipmyn® effectively neutralized 3 × LD_{50} of the venom from this lineage.

Although Antivipmyn® could recognize the pooled venoms of juveniles and adults from most lineages by ELISA, the juvenile *C. basiliscus* venom was not fully recognized under the tested conditions (Supplementary Fig. S18). Furthermore, when the neutralization capacity of the antivenom was expressed as milligrams of antivenom that neutralize 1 mg of venom (mgAV/mgV), the juvenile *C. basiliscus* venom was one of the venoms that required a higher amount of antivenom compared to other venoms (Table 3). However, when the ED_{50} was analyzed in terms of the number of median lethal doses (LD_{50}) neutralized, one vial of Antivipmyn® would have the capacity to neutralize 1569 LD_{50} of the juvenile *C. basiliscus* venom, but only 145 LD_{50} of the adult *C. basiliscus* venom. On the other hand, despite similar ELISA titers for the venom of juvenile *C. m. nigrescens* compared to other venoms, this venom was the least neutralized by Antivipmyn®. Additionally, the hind limb spastic paralysis in mice induced by venoms containing MYO (including the pooled venoms of the juveniles *C. basiliscus* and *C. m. nigrescens*) was not abolished by Antivipmyn®, in agreement with previous reports (Borja et al., 2018b).

Enzyme immunoassays, such as ELISA, have been utilized to evaluate antivenom recognition of snake venom components. While some antivenoms show a good correlation between ELISA results and neutralization of lethality in mice, others do not. The latter may result from antivenoms recognizing highly immunogenic but toxicologically irrelevant venom components (Gutiérrez et al., 2021b). Given that the venom pool of the juvenile *C. m. nigrescens* contained >60 % of MYO, a possible explanation for the good recognition but poor neutralization of this venom could be that although the antivenom recognized most toxins, MYO -the most abundant and likely one of the most lethal components- is not fully neutralized. Antivenomics analyses are required to identify toxins poorly recognized by Antivipmyn® (Teixeira-Araújo et al., 2017).

5. Conclusions

Our results demonstrate that, although eighteen toxin families constitute the venom of five lineages from the *C. molossus* complex, four toxin families -PLA_2, MYO, SVMP, and SVSP- dominate the venom composition. However, the number of toxins within these four toxin families and their abundance drastically varied across and within lineages (with intraspecific variations associated with snake size), affecting venom bioactivities.

Our findings also indicate that, in general, Antivipmyn® is effective in recognizing and neutralizing the venom variants within the *C. molossus* complex. However, MYO-rich venoms are less effectively recognized and neutralized. It is important to note that due to the wide geographical distribution of most lineages within the *C. molossus* complex, additional venom components and/or different patterns of variation could be present in other populations, as previously described for *C. basiliscus* (Colis-Torres et al., 2022).

The results of this study open challenging questions for future research to understand the evolutionary processes driving rattlesnake venom variation and the molecular mechanisms involved.

Supplementary data to this article can be found online at https://doi.org/10.1016/j.cbpc.2025.110129.

CRediT authorship contribution statement

Miguel Borja: Writing – review & editing, Writing – original draft, Visualization, Validation, Supervision, Software, Resources, Project administration, Methodology, Investigation, Funding acquisition, Formal analysis, Data curation, Conceptualization. **Gamaliel Castañeda-Gaytán:** Writing – review & editing, Supervision, Investigation, Funding acquisition, Conceptualization. **Alejandro Alagón:** Writing – review & editing, Validation, Investigation, Funding acquisition, Formal analysis, Conceptualization. **Jason L. Strickland:** Writing – review & editing, Funding acquisition, Conceptualization. **Christopher L. Parkinson:** Writing – review & editing, Funding acquisition, Conceptualization. **Areli Gutiérrez-Martínez:** Visualization, Data curation, Conceptualization. **Bruno Rodriguez-López:** Data curation, Conceptualization. **Vanessa Zarzosa:** Writing – review & editing, Visualization, Methodology, Investigation, Data curation. **Bruno Lomonte:** Writing – review & editing, Methodology, Investigation, Formal analysis, Data curation. **Anthony J. Saviola:** Writing – review & editing, Validation, Methodology, Formal analysis, Data curation. **Julián Fernández:** Writing – review & editing, Software, Formal analysis, Data curation. **Cara F. Smith:** Writing – review & editing, Software, Methodology, Investigation, Data curation. **Kirk C. Hansen:** Software, Methodology, Data curation. **Armando Pérez-Robles:** Methodology, Investigation. **Sebastián Castañeda-Pérez:** Visualization, Investigation, Data curation. **Samuel R. Hirst:** Writing – review & editing, Methodology. **Felipe Olvera-Rodríguez:** Methodology. **Leonardo Fernández-Badillo:** Writing – review & editing, Methodology. **Jesús Sigala:** Writing – review & editing, Methodology. **Jason Jones:** Resources, Methodology. **Carlos Montaño-Ruvalcaba:** Resources. **Ricardo Ramírez-Chaparro:** Resources. **Mark J. Margres:** Writing – review & editing, Methodology. **Gerardo Acosta-Campaña:** Resources. **Edgar Neri-Castro:** Writing – review & editing, Writing – original draft, Visualization, Validation, Supervision, Software, Resources, Project administration, Methodology, Investigation, Funding acquisition, Formal analysis, Data curation, Conceptualization.

Funding

This work was supported by CONAHCYT (FORDECYT-PRONACES/1715618/2020, and PRONAII 303045).

Declaration of competing interest

The authors declare that they have no known competing financial interests or personal relationships that could have appeared to influence the work reported in this paper.

Acknowledgments

The authors thank Sara Valenzuela, Jorge Becerra, Fernando Martínez, Juan Castañeda Gaytán, Rúben Carbajal Márquez, Nallely Morales Capellán, Peter Heimes, Jorge Jiménez Canale, Lizbeth Hernández Tiburcio, Edwin Pérez Bautista, Francisco Ramírez Piña, Judith Alvarez, Estefania Salcedo, Juliana Galindo and Miguel García for their assistance in the work field. We would like to thank Rhett M. Rautsaw for reviewing the manuscripts. The author, Edgar Enrique Neri Castro, gratefully acknowledges the support of the "Investigadores por Mexico" program of SECIHTI, under which he is conducting research for project 2024. In addition, we would like to thank the CONAHCYT for supporting the scholarship grant to the postgraduate students Areli Gutierrez-Martínez (No. 1241150) and Bruno Rodriguez López (No. 785652).

Data availability

Data will be made available on request.

References

Alape-Girón, A., Sanz, L., Escolano, J., Flores-Díaz, M., Madrigal, M., Sasa, M., Calvete, J. J., 2008. Snake venomics of the lancehead pitviper *Bothrops asper*. Geographic, individual, and ontogenetic variations. J. Proteome Res. 7, 3556–3571. https://doi.org/10.1021/pr800332p.

Anderson, C.G., Greenbaum, E., 2012. Phylogeography of northern populations of the black-tailed rattlesnake (*Crotalus molossus* Baird and Girard, 1853), with the revalidation of *C. ornatus* Hallowell, 1854. Herpetol. Monogr. 26, 19–57. https://doi.org/10.1655/HERPMONOGRAPHS-D-11-00012.1.

Andrade, D.V., Abe, A.S., 1999. Relationship of venom ontogeny and diet in *Bothrops*. Herpetologica 55 (2), 200–204.

Arnaud, G., García-de León, F.J., Beltrán, L.F., Carbajal-Saucedo, A., 2021. Proteomic comparison of adult and juvenile Santa Catalina rattlesnake (*Crotalus catalinensis*) venom. Toxicon 193, 55–62. https://doi.org/10.1016/j.toxicon.2021.01.014.

Arnaud-Franco, G., Cordero-Tapia, A., Ortíz-Ávila, V., Moctezuma-González, C.L., Tejocote-Pérez, M., Carbajal-Saucedo, A., 2018. Comparison of biological and biochemical characteristics of venom from rattlesnakes in the southern Baja California Peninsula. Toxicon 148, 197–201. https://doi.org/10.1016/j.toxicon.2018.04.030.

Balchan, N.R., Smith, C.F., Mackessy, S.P., 2024. A plethora of rodents: rattlesnake predators generate unanticipated patterns of venom resistance in a grassland ecosystem. Toxicon X 21. https://doi.org/10.1016/j.toxcx.2023.100179.

Balderas-Valdivia, C.J., Barreto-Oble, D., Madrid-Sotelo, C.A., 2009. Contribución a la historia natural de *Crotalus molossus*. In: Lot, A., Cano-Santana, Z. (Eds.), Biodiversidad del Ecosistema del Pedregal de San Ángel. D.F. UNAM, México, pp. 363–369.

Bonfim, V.L., Toyama, M.H., Novello, J.C., Hyslop, S., Oliveira, C.R.B., Rodrigues-Simioni, L., Marangoni, S., 2001. Isolation and enzymatic characterization of a basic phospholipase A2 from *Bothrops jararacussu* snake venom. J. Protein Chem. 20, 239–245. https://doi.org/10.1023/A:1010956126585.

Borja, M., Lazcano, D., Martínez-Romero, G., Morlett, J., Sánchez, E., Cepeda-Nieto, A.C., Garza-García, Y., Zugasti-Cruz, A., 2013. Intra-specific variation in the protein composition and proteolytic activity of venom of *Crotalus lepidus morulus* from the Northeast of Mexico. Copeia 707–716. https://doi.org/10.1643/OT-13-005.

Borja, M., Neri-Castro, E., Castañeda-Gaytán, G., Strickland, J.L., Parkinson, C.L., Castañeda-Gaytán, J., Ponce-López, R., Lomonte, B., Olvera-Rodríguez, A., Alagón, A., Pérez-Morales, R., 2018a. Biological and proteolytic variation in the venom of *Crotalus scutulatus scutulatus* from Mexico. Toxins (Basel) 10, 1–19. https://doi.org/10.3390/toxins10010035.

Borja, M., Neri-Castro, E., Pérez-Morales, R., Strickland, J.L., Ponce-López, R., Parkinson, C.L., Espinosa-Fematt, J., Sáenz-Mata, J., Flores-Martínez, E., Alagón, A., Castañeda-Gaytán, G., 2018b. Ontogenetic change in the venom of Mexican Blacktailed rattlesnakes (*Crotalus molossus nigrescens*). Toxins (Basel) 10. https://doi.org/10.3390/toxins10120501.

Borja, M., Neri-Castro, E., Gutiérrez-Martínez, A., Bledsoe, R., Zarzosa, V., Rodriguez-López, B., Strickland, J.L., Becerra-López, J., Valenzuela-Ceballos, S., Parkinson, C. L., Alagón, A., Castañeda-Gaytán, G., 2023. Ontogenetic change in the venom composition of one Mexican Black-tailed rattlesnake (*Crotalus molossus nigrescens*) from Durango, Mexico. Toxicon 234. https://doi.org/10.1016/j.toxicon.2023.107280.

Bosak, A.R., Ruha, A.M., Graeme, K.A., 2014. A case of neurotoxicity following envenomation by the sidewinder rattlesnake, *Crotalus cerastes*. J. Med. Toxicol. 10, 229–231. https://doi.org/10.1007/s13181-013-0373-0.

Calvete, J.J., Juárez, P., Sanz, L., 2007. Snake venomics. Strategy and applications. Journal of Mass Spectrometry 1405–1414. https://doi.org/10.1002/jms.1242.

Calvete, J.J., Lomonte, B., Saviola, A.J., Calderón Celis, F., Ruiz Encinar, J., 2023. Quantification of snake venom proteomes by mass spectrometry-considerations and perspectives. Mass Spectrom. Rev. https://doi.org/10.1002/mas.21850.

Carbajal-Márquez, R.A., Sigala-Rodríguez, J.J., Reyes-Velasco, J., Jones, J.M., Montaño-Ruvalcaba, C., Fernández-Badillo, L., Borja-Jiménez, J.M., 2023. New dietary records for three species in the *Crotalus molossus* species complex (Serpentes: Viperidae). Phyllomedusa 22, 81–86. https://doi.org/10.11606/issn.2316-9079.v22i1p81-86.

Casewell, N.R., Jackson, T.N.W., Laustsen, A.H., Sunagar, K., 2020. Causes and consequences of snake venom variation. Trends Pharmacol. Sci. 41, 570–581. https://doi.org/10.1016/j.tips.2020.05.006.

Castro, E.N., Lomonte, B., del Carmen Gutiérrez, M., Alagón, A., Gutiérrez, J.M., 2013. Intraspecies variation in the venom of the rattlesnake *Crotalus simus* from Mexico: different expression of crotoxin results in highly variable toxicity in the venoms of three subspecies. J. Proteomics 87, 103–121. https://doi.org/10.1016/j.jprot.2013.05.024.

Cipriani, V., Debono, J., Goldenberg, J., Jackson, T.N.W., Arbuckle, K., Dobson, J., Koludarov, I., Li, B., Hay, C., Dunstan, N., Allen, L., Hendrikx, I., Kwok, H.F., Fry, B. G., 2017. Correlation between ontogenetic dietary shifts and venom variation in Australian brown snakes (*Pseudonaja*). Comparative Biochemistry and Physiology Part - C: Toxicology and Pharmacology 197, 53–60. https://doi.org/10.1016/j.cbpc.2017.04.007.

Colis-Torres, A., Neri-Castro, E., Strickland, J.L., Olvera-Rodríguez, A., Borja, M., Calvete, J., Jones, J., Parkinson, C.L., Bañuelos, J., López de León, J., Alagón, A., 2022. Intraspecific venom variation of Mexican west coast rattlesnakes (*Crotalus basiliscus*) and its implications for antivenom production. Biochimie 192, 111–124. https://doi.org/10.1016/j.biochi.2021.10.006.

Dantas Almeida, D., Louis Viala, V., Nachtigall, P.G., Broe, M., Lisle Gibbs, H., Maria De Toledo Serrano, S., Moura-Da-Silva, A.M., Ho, P.L., Yutaka Nishiyama-Jr, M., Junqueira-De-Azevedo, I.L.M., 2021. Tracking the recruitment and evolution of snake toxins using the evolutionary context provided by the *Bothrops jararaca* genome, 118. https://doi.org/10.1073/pnas.2015159118/-/DCSupplemental.

Debono, J., Bos, M.H.A., Do, M.S., Fry, B.G., 2019a. Clinical implications of coagulotoxic variations in Mamushi (Viperidae: Gloydius) snake venoms. Comp. Biochem. Physiol., Part C: Toxicol. Pharmacol. 225, 108567. https://doi.org/10.1016/J.CBPC.2019.108567.

Debono, J., Bos, M.H.A., Frank, N., Fry, B., 2019b. Clinical implications of differential antivenom efficacy in neutralising coagulotoxicity produced by venoms from species within the arboreal viperid snake genus Trimeresurus. Toxicol. Lett. 316, 35–48. https://doi.org/10.1016/J.TOXLET.2019.09.003.

Dowell, N.L., Giorgianni, M.W., Kassner, V.A., Selegue, J.E., Sanchez, E.E., Carroll, S.B., 2016. The deep origin and recent loss of venom toxin genes in rattlesnakes. Curr. Biol. 26, 2434–2445. https://doi.org/10.1016/j.cub.2016.07.038.

Dowell, N.L., Giorgianni, M.W., Griffin, S., Kassner, V.A., Selegue, J.E., Sanchez, E.E., Carroll, S.B., 2018. Extremely divergent haplotypes in two toxin gene complexes encode alternative venom types within rattlesnake species. Curr. Biol. 28, 1016–1026 e4. https://doi.org/10.1016/j.cub.2018.02.031.

Durban, J., Pérez, A., Sanz, L., Gómez, A., Bonilla, F., Rodríguez, S., Chacón, D., Sasa, M., Angulo, Y., Gutiérrez, J.M., Calvete, J.J., 2013. Integrated "omics" profiling indicates that miRNAs are modulators of the ontogenetic venom composition shift in the Central American rattlesnake, *Crotalus simus simus*. BMC Genomics 14, 1–17. https://doi.org/10.1186/1471-2164-14-234.

Durban, J., Sanz, L., Trevisan-Silva, D., Neri-Castro, E., Alagón, A., Calvete, J.J., 2017. Integrated venomics and venom gland transcriptome analysis of juvenile and adult Mexican rattlesnakes *Crotalus simus*, *C. tzabcan*, and *C. culminatus* revealed miRNA-modulated ontogenetic shifts. J. Proteome Res. 16, 3370–3390. https://doi.org/10.1021/acs.jproteome.7b00414.

Ernst, C.H., Ernst, E.M., 2011. Venomous Reptiles of the United States, Canada, and Northern Mexico. Johns Hopkins University Press.

Fernández, J., Gutiérrez, J.M., Angulo, Y., Sanz, L., Juárez, P., Calvete, J.J., Lomonte, B., 2010. Isolation of an acidic phospholipase A2 from the venom of the snake *Bothrops asper* of Costa Rica: biochemical and toxicological characterization. Biochimie 92, 273–283. https://doi.org/10.1016/j.biochi.2009.12.006.

Franco-Servín, C., Neri-Castro, E., Bénard-Valle, M., Alagón, A., Rosales-García, R.A., Guerrero-Alba, R., Poblano-Sánchez, J.E., Silva-Briano, M., Guerrero-Barrera, A.L., Sigala-Rodríguez, J.J., 2021. Biological and biochemical characterization of Coronado island rattlesnake (*Crotalus helleri caliginis*) venom and antivenom neutralization. Toxins (Basel) 13. https://doi.org/10.3390/toxins13080582.

Funk, R.S., 1964. On the food of *Crotalus m. molossus*. Herpetologica 20, 134.

Giorgianni, M.W., Dowell, N.L., Griffin, S., Kassner, V.A., Selegue, J.E., Carroll, S.B., 2020. The origin and diversification of a novel protein family in venomous snakes. Proc. Natl. Acad. Sci. U. S. A. 117, 10911–10920. https://doi.org/10.1073/pnas.1920011117.

Gopalan, S.S., Perry, B.W., Francioli, Y.Z., Schield, D.R., Guss, H.D., Bernstein, J.M., Ballard, K., Smith, C.F., Saviola, A.J., Adams, R.H., Mackessy, S.P., Castoe, T.A., 2024. Diverse gene regulatory mechanisms alter rattlesnake venom gene expression at fine evolutionary scales. Genome Biol. Evol. https://doi.org/10.1093/gbe/evae110.

Grabowsky, E.R., Mackessy, S.P., 2019. Predator-prey interactions and venom composition in a high elevation lizard specialist, *Crotalus pricei* (twin-spotted rattlesnake). Toxicon 170, 29–40. https://doi.org/10.1016/j.toxicon.2019.09.011.

Grabowsky, E.R., Saviola, A.J., Alvarado-Díaz, J., Mascareñas, A.Q., Hansen, K.C., Yates, J.R., Mackessy, S.P., 2023. Montane rattlesnakes in Mexico: venoms of *Crotalus tancitarensis* and related species within the *Crotalus intermedius* group. Toxins (Basel) 15. https://doi.org/10.3390/toxins15010072.

Gren, E.C.K., Kelln, W., Person, C., McCabe, J.G., Kornhauser, R., Hart, A.J., Erbas-White, K., Pompe, L.R., Hayes, W.K., 2017. Geographic variation of venom composition and neurotoxicity in the rattlesnakes *Crotalus oreganus* and *C. helleri*: assessing the potential roles of selection and neutral evolutionary processes in shaping venom variation. The Biology of Rattlesnakes II, 228–252.

Guadarrama-Martínez, A., Neri-Castro, E., Boyer, L., Alagón, A., 2024. Variability in antivenom neutralization of Mexican viperid snake venoms. PLoS Negl. Trop. Dis. 18. https://doi.org/10.1371/journal.pntd.0012152.

Guércio, R.A.P., Shevchenko, Anna, Shevchenko, Andrej, López-Lozano, J.L., Paba, J., Sousa, M.V., Ricart, C.A.O., 2006. Ontogenetic variations in the venom proteome of the Amazonian snake *Bothrops atrox*. Proteome Sci. 4, 1–14. https://doi.org/10.1186/1477-5956-4-11.

Gutiérrez, J., Rucavado, A., Escalante, T., 2009. Snake venom metalloproteinases. Biological roles and participation in the pathophysiology of envenomation. In: Mackessy, S.P. (Ed.), Handbook of Venoms and Toxins of Reptiles, 1st ed. CRC Press, Boca Raton, FL, USA.

Gutiérrez, J.M., Escalante, T., Rucavado, A., Herrera, C., 2016. Hemorrhage caused by snake venom metalloproteinases: a journey of discovery and understanding. Toxins (Basel) 8. https://doi.org/10.3390/toxins8040093.

Gutiérrez, J.M., Calvete, J.J., Habib, A.G., Harrison, R.A., Williams, D.J., Warrell, D.A., 2017a. Snakebite envenoming. Nat. Rev. Dis. Primers. 3. https://doi.org/10.1038/NRDP.2017.63.

Gutiérrez, J.M., Solano, G., Pla, D., Herrera, M., Segura, Á., Vargas, M., Villalta, M., Sánchez, A., Sanz, L., Lomonte, B., León, G., Calvete, J.J., 2017b. Preclinical evaluation of the efficacy of antivenoms for snakebite envenoming: state-of-the-art and challenges ahead. Toxins (Basel) 9. https://doi.org/10.3390/toxins9050163.

Gutiérrez, J.M., Albulescu, L.O., Clare, R.H., Casewell, N.R., Abd El-Aziz, T.M., Escalante, T., Rucavado, A., 2021a. The search for natural and synthetic inhibitors that would complement antivenoms as therapeutics for snakebite envenoming. Toxins (Basel). https://doi.org/10.3390/toxins13070451.

Gutiérrez, J.M., Vargas, M., Segura, Á., Herrera, M., Villalta, M., Solano, G., Sánchez, A., Herrera, C., León, G., 2021b. In vitro tests for assessing the neutralizing ability of snake antivenoms: toward the 3Rs principles. Front. Immunol. 11. https://doi.org/10.3389/fimmu.2020.617429.

Hardy, D.L., Jeter, M., Corrigan, J.J., 1982. Envenomation by the northern blacktail rattlesnake (*Crotalus molossus molossus*): report of two cases and the vitro effects of the venom on fibrinolysis and platelet aggregation. Toxicon 20, 487–493. https://doi.org/10.1016/0041-0101(82)90012-5.

Hirst, S.R., Rautsaw, R.M., VanHorn, C.M., Beer, M.A., McDonald, P.J., Rosales-García, R.A., Lopez, B.R., Rubio Rincón, A., Franz-Chávez, H., Vásquez-Cruz, V., Kelly-Hernández, A., Storfer, A., Borja, M., Castañeda-Gaytán, G., Frandsen, P.B., Parkinson, C.L., Strickland, J.L., Margres, M.J., 2024. Where the 'ruber' meets the road: using the genome of the red diamond rattlesnake to unravel the evolutionary processes driving venom evolution. Genome Biol. Evol. https://doi.org/10.1093/gbe/evae198.

Hogan, M.P., Holding, M.L., Nystrom, G.S., Colston, T.J., Bartlett, D.A., Mason, A.J., Ellsworth ID, S.A., Rautsaw, R.M., Lawrence, K.C., Strickland, J.L., He, B., Fraser, P. I., Margres ID, M.J., Gilbert ID, D.M., Lisle Gibbs, H.I., Parkinson, C.L., Rokyta, D.R., 2024. The genetic regulatory architecture and epigenomic basis for age-related changes in rattlesnake venom, 121. https://doi.org/10.1073/pnas.

Holding, M.L., Strickland, J.L., Rautsaw, R.M., Hofmann, E.P., Mason, A.J., Hogan, M.P., Nystrom, G.S., Ellsworth, S.A., Colston, T.J., Borja, M., Castañeda-Gaytán, G., Grünwald, C.I., Jones, J.M., Freitas-De-Sousa, L.A., Viala, V.L., Margres, M.J., Hingst-Zaher, E., Junqueira-De-Azevedo, I.L.M., Moura-Da-Silva, A.M., Grazziotin, F. G., Lisle Gibbs, H., Rokyta, D.R., Parkinson, C.L., 2021. Phylogenetically diverse diets favor more complex venoms in North American pitvipers. Proc. Natl. Acad. Sci. U. S. A. 118. https://doi.org/10.1073/pnas.2015579118.

Holzer, M., Mackessy, S.P., 1996. An aqueous endpoint assay of snake venom phospholipase A2. Toxicon 34, 1149–1155. https://doi.org/10.1016/0041-0101(96)00057-8.

Jimenez-Canale, J., Navarro-Lopez, R., Huerta-Ocampo, J.A., Burgara-Estrella, A.J., Encarnacion-Guevara, S., Silva-Campa, E., Velazquez-Contreras, F.E., Sarabia-Sainz, J.A., 2024. Exploring the protein profile and biological activity of *Crotalus molossus* venom against *E. coli*, *P. aeruginosa* and *S. aureus* bacteria and T47D breast carcinoma cells. Toxicon 249. https://doi.org/10.1016/j.toxicon.2024.108036.

Jiménez-Charris, E., Montealegre-Sánchez, L., Solano-Redondo, L., Castro-Herrera, F., Fierro-Pérez, L., Lomonte, B., 2016. Divergent functional profiles of acidic and basic phospholipases A2 in the venom of the snake *Porthidium lansbergii lansbergii*. Toxicon 119, 289–298. https://doi.org/10.1016/j.toxicon.2016.07.006.

Keyler, D.E., Saini, V., O'Shea, M., Gee, J., Smith, C.F., Mackessy, S.P., 2020. Crotalus oreganus concolor: envenomation case with venom analysis and a diagnostic conundrum of myoneurologic symptoms. Wilderness Environ. Med. 31, 220–225. https://doi.org/10.1016/j.wem.2019.12.007.

Klauber, L.M., 1972. Rattlesnakes: Their Habits, Life Histories and Influence on Mankind, 2nd edition. University of California Press, Berkeley and Los Angeles. 1533 pp.

Kong, A.T., Leprevost, F.V., Avtonomov, D.M., Mellacheruvu, D., Nesvizhskii, A.I., 2017. MSFragger: ultrafast and comprehensive peptide identification in mass spectrometry-based proteomics. Nat. Methods 14, 513–520. https://doi.org/10.1038/nmeth.4256.

Lomonte, B., 2023. Lys49 myotoxins, secreted phospholipase A2-like proteins of viperid venoms: a comprehensive review. Toxicon 224, 107024. https://doi.org/10.1016/j.toxicon.2023.107024.

Lomonte, B., Angulo, Y., Sasa, M., Gutiérrez, J.M., Rica, D.C., José, S., Rica, C., 2009. The phospholipase A2 homologues of snake venoms: biological activities and their possible adaptive roles. Protein Pept. Lett. 16 (8), 860–876. https://doi.org/10.2174/092986609788923356, 2009. PMID: 19689412.

Lorke, D., 1983. A new approach to practical acute toxicity testing. Arch. Toxicol. 54, 275–287. https://doi.org/10.1007/BF01234480.

Macedo, J.K.A., Fox, J.W., 2016. Biological activities and assays of the snake venom metalloproteinases (SVMPs). In: Gopalakrishnakone, P., Calvete, J. (Eds.), Venom Genomics and Proteomics, Toxinology. Springer, Dordrecht. https://doi.org/10.1007/978-94-007-6416-3_21.

Mackessy, S.P., 2010a. Evolutionary trends in venom composition in the Western rattlesnakes (*Crotalus viridis* sensu lato): toxicity vs. tenderizers. Toxicon 55, 1463–1474. https://doi.org/10.1016/j.toxicon.2010.02.028.

Mackessy, S.P., 2010b. Thrombin-like enzymes in snake venoms. In: Kini, R., Clemetson, K., Markland, F., McLane, M., Morita, T. (Eds.), Toxins and Hemostasis. Springer, Dordrecht. https://doi.org/10.1007/978-90-481-9295-3_30.

Mackessy, S.P., Saviola, A.J., 2016. Understanding biological roles of venoms among the Caenophidia: the importance of rear-fanged snakes. Integr. Comp. Biol. 56, 1004–1021. https://doi.org/10.1093/icb/icw110.

Mackessy, S.P., Williams, K., Ashton, K.G., 2003. Ontogenetic variation in venom composition and diet of *Crotalus oreganus concolor*. A case of venom paedomorphosis? Copeia 2003, 769–782. https://doi.org/10.1643/HA03-037.1.

Mackessy, S.P., Sixberry, N.M., Heyborne, W.H., Fritts, T., 2006. Venom of the brown treesnake, *Boiga irregularis*: ontogenetic shifts and taxa-specific toxicity. Toxicon 47, 537–548. https://doi.org/10.1016/j.toxicon.2006.01.007.

Mackessy, S.P., Leroy, J., Mociño-Deloya, E., Setser, K., Bryson, R.W., Saviola, A.J., 2018. Venom ontogeny in the Mexican lance-headed rattlesnake (*Crotalus polystictus*). Toxins (Basel) 10. https://doi.org/10.3390/toxins10070271.

Margres, M.J., Wray, K.P., Seavy, M., McGivern, J.J., Sanader, D., Rokyta, D.R., 2015. Phenotypic integration in the feeding system of the eastern diamondback rattlesnake (*Crotalus adamanteus*). Mol. Ecol. 24, 3405–3420. https://doi.org/10.1111/mec.13240.

Margres, M.J., Bigelow, A.T., Lemmon, E.M., Lemmon, A.R., Rokyta, D.R., 2017. Selection to increase expression, not sequence diversity, precedes gene family origin and expansion in rattlesnake venom. Genetics 206, 1569–1580. https://doi.org/10.1534/genetics.117.202655.

Margres, M.J., Rautsaw, R.M., Strickland, J.L., Mason, A.J., Schramer, T.D., Hofmann, E. P., Stiers, E., Ellsworth, S.A., Nystrom, G.S., Hogan, M.P., Bartlett, D.A., Colston, T. J., Gilbert, D.M., Rokyta, D.R., Parkinson, C.L., 2021a. The tiger rattlesnake genome reveals a complex genotype underlying a simple venom phenotype. Proc. Natl. Acad. Sci. 118, e2014634118. https://doi.org/10.1073/pnas.2014634118.

Margres, M.J., Wray, K.P., Sanader, D., McDonald, P.J., Trumbull, L.M., Patton, A.H., Rokyta, D.R., 2021b. Varying intensities of introgression obscure incipient venom-associated speciation in the timber rattlesnake (*Crotalus horridus*). Toxins (Basel) 13. https://doi.org/10.3390/toxins13110782.

Martínez-Romero, G., Rucavado, A., Lazcano, D., Gutiérrez, J.M., Borja, M., Lomonte, B., Garza-García, Y., Zugasti-Cruz, A., 2013. Comparison of venom composition and biological activities of the subspecies *Crotalus lepidus lepidus*, *Crotalus lepidus klauberi* and *Crotalus lepidus morulus* from Mexico. Toxicon 71, 84–95. https://doi.org/10.1016/j.toxicon.2013.05.006.

Massey, D.J., Calvete, J.J., Sánchez, E.E., Sanz, L., Richards, K., Curtis, R., Boesen, K., 2012. Venom variability and envenoming severity outcomes of the *Crotalus scutulatus scutulatus* (Mojave rattlesnake) from Southern Arizona. J. Proteomics 75, 2576–2587. https://doi.org/10.1016/j.jprot.2012.02.035.

Melani, R.D., Goto-Silva, L., Nogueira, F.C.S., Junqueira, M., Domont, G.B., 2016. Shotgun approaches for venom analysis. In: Venom Genomics and Proteomics. Springer, Netherlands, pp. 367–380. https://doi.org/10.1007/978-94-007-6416-3_26.

Meléndez-Martínez, D., Plenge-Tellechea, L.F., Gatica-Colima, A., Cruz-Pérez, M.S., Aguilar-Yáñez, J.M., Licona-Cassani, C., 2020. Functional mining of the *Crotalus* spp. venom protease repertoire reveals potential for chronic wound therapeutics. Molecules 25. https://doi.org/10.3390/molecules25153401.

Meyer, S., Hartmann, F., Stein, P., Lenherr, R., Fuchs, J., Spahn, D.R., 2017. Massive coagulopathy caused by the bite of a *Crotalus basiliscus* snake. Anaesth Cases 5, 60–65. https://doi.org/10.21466/ac.fcoabbc.2017.

Mora-Obando, D., Fernández, J., Montecucco, C., Gutiérrez, J.M., Lomonte, B., 2014. Synergism between basic Asp49 and Lys49 phospholipase A2 myotoxins of viperid snake venom in vitro and in vivo. PloS One 9. https://doi.org/10.1371/journal.pone.0109846.

Mora-Obando, D., Salazar-Valenzuela, D., Pla, D., Lomonte, B., Guerrero-Vargas, J.A., Ayerbe, S., Gibbs, H.L., Calvete, J.J., 2020. Venom variation in *Bothrops asper* lineages from North-Western South America. J. Proteomics 229. https://doi.org/10.1016/j.jprot.2020.103945.

Muñoz-Mora, V.H., Suárez-atilano, M., Maltagliati, F., Ramírez-corona, F., Carbajal-saucedo, A., Percino-daniel, R., 2022. A tale about vipers' tails: phylogeography of black-tailed rattlesnakes, 153, 141–153. https://doi.org/10.3897/herpetozoa.35.e84297.

Myers, E.A., Rautsaw, R.M., Borja, M., Jones, J., Grünwald, C.I., Holding, M.L., Grazziotin, F.G., Parkinson, C.L., 2024. Phylogenomic discordance is driven by widespread introgression and incomplete lineage sorting during rapid species diversification within rattlesnakes (Viperidae: *Crotalus* and *Sistrurus*). Systematic Biology 2024, syae018. https://doi.org/10.1093/sysbio/syae018.

Neri-Castro, E., Bénard-Valle, M., Gil, G., Borja, M., León, J.L. de, Alagón, A., 2020. Venomous snakes in Mexico: a review of the study of venoms, antivenom and epidemiology. Revista Latinoamericana de Herpetologia 3, 05–22.

Neri-Castro, E., Bénard-Valle, M., León, J.L. de, Boyer, L., Alagón, A., 2021. Envenomations by reptiles in Mexico. In: Kini, R., Clemetson, K., Markland, F., McLane, M., Morita, T. (Eds.), Handbook of Venoms and Toxins of Reptiles, 2nd edition. CRC Press.

Neri-Castro, E., Zarzosa, V., Colis-Torres, A., Fry, B.G., Olvera-Rodríguez, A., Jones, J., Reyes-Velasco, J., Zamudio, F., Borja, M., Alagón, A., Lomonte, B., 2022. Proteomic and toxicological characterization of the venoms of the most enigmatic group of rattlesnakes: the long-tailed rattlesnakes. Biochimie 202, 226–236. https://doi.org/10.1016/j.biochi.2022.08.015.

Núñez, V., Cid, P., Sanz, L., De La Torre, P., Angulo, Y., Lomonte, B., Gutiérrez, J.M., Calvete, J.J., 2009. Snake venomics and antivenomics of *Bothrops atrox* venoms from Colombia and the Amazon regions of Brazil, Perú and Ecuador suggest the occurrence of geographic variation of venom phenotype by a trend towards paedomorphism. J. Proteomics 73, 57–78. https://doi.org/10.1016/j.jprot.2009.07.013.

Oliveira, A.L., Viegas, M.F., da Silva, S.L., Soares, A.M., Ramos, M.J., Fernandes, P.A., 2022. The chemistry of snake venom and its medicinal potential. Nat. Rev. Chem. https://doi.org/10.1038/s41570-022-00393-7.

Ponce-López, R., Neri-Castro, E., Borja, M., Strickland, J.L., Alagón, A., 2020. Neutralizing potency and immunochemical evaluation of an anti-*Crotalus mictlantecuhtli* experimental serum. Toxicon 187, 171–180. https://doi.org/10.1016/j.toxicon.2020.08.026.

Ponce-López, R., Neri-Castro, E., Olvera-Rodríguez, F., Sánchez, E.E., Alagón, A., Olvera-Rodríguez, A., 2021. Neutralization of crotamine by polyclonal antibodies generated against two whole rattlesnake venoms and a novel recombinant fusion protein. Toxicon 197, 70–78. https://doi.org/10.1016/j.toxicon.2021.04.005.

Pozas-Ocampo, I.F., Carbajal-Saucedo, A., Gatica-Colima, A.B., Cordero-Tapia, A., Arnaud-Franco, G., 2020. Toxicological comparison of *Crotalus ruber lucasensis* venom from different ecoregions of the Baja California Peninsula. Toxicon 187, 111–115. https://doi.org/10.1016/j.toxicon.2020.08.029.

Rael, E.D., Rivas, J.Z., Chen, T., Maddux, N., Huizar, E., Lieb, C.S., 1997. Differences in fibrinolysis and complement inactivation by venom from different Northern Blacktailed rattlesnakes (*Crotalus molossus molossus*). Toxicon 35, 505–513. https://doi.org/10.1016/S0041-0101(96)00139-0.

Rivas Mercado, E., Neri Castro, E., Bénard Valle, M., Rucavado-Romero, A., Olvera Rodríguez, A., Zamudio Zuñiga, F., Alagón Cano, A., Garza Ocañas, L., 2020. Disintegrins extracted from totonacan rattlesnake (*Crotalus totonacus*) venom and their anti-adhesive and anti-migration effects on MDA-MB-231 and HMEC-1 cells. Toxicol. In Vitro 65, 104809. https://doi.org/10.1016/j.tiv.2020.104809.

Sánchez, E.E., Galán, J.A., Perez, J.C., Rodríguez-Acosta, A., Chase, P.B., Pérez, J.C., 2003. The efficacy of two antivenoms against the venom of North American snakes. Toxicon 41, 357–365. https://doi.org/10.1016/S0041-0101(02)00330-6.

Sanchez, E.F., Flores-Ortiz, R.J., Alvarenga, V.G., Eble, J.A., 2017. Direct fibrinolytic snake venom metalloproteinases affecting hemostasis: structural, biochemical features and therapeutic potential. Toxins (Basel) 9. https://doi.org/10.3390/toxins9120392.

Sánchez, M., Solano, G., Vargas, M., Reta-Mares, F., Neri-Castro, É., Alagón, A., Sánchez, A., Villalta, M., León, G., Segura, Á., 2020. Toxicological profile of medically relevant *Crotalus* species from Mexico and their neutralization by a *Crotalus basiliscus/Bothrops asper* antivenom. Toxicon 179, 92–100. https://doi.org/10.1016/j.toxicon.2020.03.006.

Saviola, A.J., Pla, D., Sanz, L., Castoe, T.A., Calvete, J.J., Mackessy, S.P., 2015. Comparative venomics of the prairie rattlesnake (*Crotalus viridis viridis*) from Colorado: identification of a novel pattern of ontogenetic changes in venom composition and assessment of the immunoreactivity of the commercial antivenom CroFab®. J. Proteomics 121, 28–43. https://doi.org/10.1016/j.jprot.2015.03.015.

Saviola, A.J., Gandara, A.J., Bryson, R.W., Mackessy, S.P., 2017. Venom phenotypes of the rock rattlesnake (*Crotalus lepidus*) and the ridge-nosed rattlesnake (*Crotalus willardi*) from México and the United States. Toxicon 138, 119–129. https://doi.org/10.1016/j.toxicon.2017.08.016.

Schield, D.R., Card, D.C., Hales, N.R., Perry, B.W., Pasquesi, G.M., Blackmon, H., Adams, R.H., Corbin, A.B., Smith, C.F., Ramesh, B., Demuth, J.P., Betrán, E., Tollis, M., Meik, J.M., Mackessy, S.P., Castoe, T.A., 2019. The origins and evolution of chromosomes, dosage compensation, and mechanisms underlying venom regulation in snakes. Genome Res. 29, 590–601. https://doi.org/10.1101/gr.240952.118.

Schonour, R.B., Huff, E.M., Holding, M.L., Claunch, N.M., Ellsworth, S.A., Hogan, M.P., Wray, K., McGivern, J., Margres, M.J., Colston, T.J., Rokyta, D.R., 2020. Gradual and discrete ontogenetic shifts in rattlesnake venom composition and assessment of hormonal and ecological correlates. Toxins (Basel) 12. https://doi.org/10.3390/toxins12100659.

Segura, Á., Herrera, M., Reta Mares, F., Jaime, C., Sánchez, A., Vargas, M., Villalta, M., Gómez, A., Gutiérrez, J.M., León, G., 2017. Proteomic, toxicological and immunogenic characterization of Mexican west-coast rattlesnake (*Crotalus basiliscus*) venom and its immunological relatedness with the venom of Central American rattlesnake (*Crotalus simus*). J. Proteomics 158, 62–72. https://doi.org/10.1016/j.jprot.2017.02.015.

Serrano, S.M.T., 2013. The long road of research on snake venom serine proteinases. Toxicon 62, 19–26. https://doi.org/10.1016/j.toxicon.2012.09.003.

Serrano, S.M.T., Maroun, R.C., 2005. Snake venom serine proteinases: sequence homology vs. substrate specificity, a paradox to be solved. Toxicon 45, 1115–1132. https://doi.org/10.1016/j.toxicon.2005.02.020.

Smith, C.F., Nikolakis, Z.L., Ivey, K., Perry, B.W., Schield, D.R., Balchan, N.R., Parker, J., Hansen, K.C., Saviola, A.J., Castoe, T.A., Mackessy, S.P., 2023. Snakes on a plain: biotic and abiotic factors determine venom compositional variation in a wide-ranging generalist rattlesnake. BMC Biol. 21. https://doi.org/10.1186/s12915-023-01626-x.

Sousa, L.F., Holding, M.L., Del-Rei, T.H.M., Rocha, M.M.T., Mourão, R.H.V., Chalkidis, H. M., Prezoto, B., Gibbs, H.L., Moura-Da-silva, A.M., 2021. Individual variability in *Bothrops atrox* snakes collected from different habitats in the Brazilian Amazon: new findings on venom composition and functionality. Toxins (Basel) 13, 1–18. https://doi.org/10.3390/toxins13110814.

Strickland, J.L., Mason, A.J., Rokyta, D.R., Parkinson, C.L., 2018a. Phenotypic variation in Mojave rattlesnake (*Crotalus scutulatus*) venom is driven by four toxin families. Toxins (Basel) 10, 1–23. https://doi.org/10.3390/toxins10040135.

Strickland, J.L., Smith, C.F., Mason, A.J., Schield, D.R., Borja, M., Castañeda-Gaytán, G., Spencer, C.L., Smith, L.L., Trápaga, A., Bouzid, N.M., Campillo-García, G., Flores-Villela, O.A., Antonio-Rangel, D., Mackessy, S.P., Castoe, T.A., Rokyta, D.R., Parkinson, C.L., 2018b. Evidence for divergent patterns of local selection driving venom variation in Mojave rattlesnakes (*Crotalus scutulatus*). Sci. Rep. 8, 1–15. https://doi.org/10.1038/s41598-018-35810-9.

Tasima, L.J., Serino-Silva, C., Hatakeyama, D.M., Nishiduka, E.S., Tashima, A.K., Sant'Anna, S.S., Grego, K.F., De Morais-Zani, K., Tanaka-Azevedo, A.M., 2020. Crotamine in *Crotalus durissus*: distribution according to subspecies and geographic origin, in captivity or nature. Journal of Venomous Animals and Toxins Including Tropical Diseases 26, 1–14. https://doi.org/10.1590/1678-9199-jvatitd-2019-0053.

Teixeira-Araújo, R., Castanheira, P., Brazil-Más, L., Pontes, F., Leitão de Araújo, M., Machado Alves, M.L., Zingali, R.B., Correa-Netto, C., 2017. Antivenomics as a tool to improve the neutralizing capacity of the crotalic antivenom: a study with crotamine. Journal of Venomous Animals and Toxins Including Tropical Diseases 23, 1–8. https://doi.org/10.1186/s40409-017-0118-7.

Tosin, O., Karina, P., Selistre-de-araujo, H.S., Helena, D., Souza, F. De, 2020. Snake Venom Metalloproteinases (SVMPs): a structure-function update. Toxicon X 7, 100052. https://doi.org/10.1016/j.toxcx.2020.100052, 2020 Jul 21. PMID: 32776002; PMCID: PMC7399193.

Uetz, P., Freed, P., Aguilar, R., Reyes, F., Kudera, J., Hošek, J., 2024. The Reptile Database. http://www.reptile-database.org.

Ullah, A., Masood, R., Ali, I., Ullah, K., Ali, H., Akbar, H., Betzel, C., 2018. Thrombin-like enzymes from snake venom: structural characterization and mechanism of action. Int. J. Biol. Macromol. 114, 788–811. https://doi.org/10.1016/j.ijbiomac.2018.03.164.

Van der Laat, M., Fernández, J., Durban, J., Villalobos, E., Camacho, E., Calvete, J.J., Lomonte, B., 2013. Amino acid sequence and biological characterization of BlatPLA2, a non-toxic acidic phospholipase A2 from the venom of the arboreal snake *Bothriechis lateralis* from Costa Rica. Toxicon 73, 71–80. https://doi.org/10.1016/j.toxicon.2013.07.008.

Vohra, R., Cantrell, F.L., Williams, S.R., 2008. Fasciculations after rattlesnake envenomations: a retrospective statewide poison control system study. Clin. Toxicol. 46, 117–121. https://doi.org/10.1080/15563650701638925.

Walzthoeni, T., Joachimiak, L.A., Rosenberger, G., Röst, H.L., Malmström, L., Leitner, A., Frydman, J., Aebersold, R., 2015 Dec. xTract: software for characterizing conformational changes of protein complexes by quantitative cross-linking mass spectrometry. Nat Methods 12 (12), 1185–1190. https://doi.org/10.1038/nmeth.3631. Epub 2015 Oct 26. PMID: 26501516; PMCID: PMC4927332.

Wang, W.J., Shih, C.H., Huang, T.F., 2004. A novel P-I class metalloproteinase with broad substrate-cleaving activity, agkislysin, from *Agkistrodon acutus* venom. Biochem. Biophys. Res. Commun. 324, 224–230. https://doi.org/10.1016/j.bbrc.2004.09.031.

Weekers, D.J.C., Alonso, L.L., Verstegen, A.X., Slagboom, J., Kool, J., 2024. Qualitative profiling of venom toxins in the venoms of several *Bothrops* species using high-throughput venomics and coagulation bioassaying. Toxins (Basel) 16, 300. https://doi.org/10.3390/toxins16070300.

Westfall, A.K., Gopalan, S.S., Perry, B.W., Adams, R.H., Saviola, A.J., MacKessy, S.P., Castoe, T.A., 2023. Single-cell heterogeneity in snake venom expression is hardwired by co-option of regulators from progressively activated pathways. Genome Biol. Evol. 15. https://doi.org/10.1093/gbe/evad109.

Wüster, W., Ferguson, J.E., Quijada-Mascareñas, J.A., Pook, C.E., Salomão, M.D.G., Thorpe, R.S., 2005. Tracing an invasion: Landbridges, refugia, and the phylogeography of the Neotropical rattlesnake (Serpentes: Viperidae: *Crotalus durissus*). Mol. Ecol. 14, 1095–1108. https://doi.org/10.1111/j.1365-294X.2005.02471.x.

Yarema, M.C., Curry, S.C., 2005. Envenomation by the northern blacktail rattlesnake (*Crotalus molossus molossus*): case report. Pediatr. Emerg. Care 21, 40–42. https://doi.org/10.1097/01.pec.0000150989.03981.06.

Youngman, N.J., Debono, J., Dobson, J.S., Zdenek, C.N., Harris, R.J., den Brouw, B. op, Coimbra, F.C.P., Naude, A., Coster, K., Sundman, E., Braun, R., Hendrikx, I., Fry, B. G., 2019. Venomous landmines: clinical implications of extreme coagulotoxic diversification and differential neutralization by antivenom of venoms within the viperid snake genus Bitis. Toxins 11, 422. https://doi.org/10.3390/TOXINS11070422, 2019, Vol. 11, Page 422.

Zancolli, G., Calvete, J.J., Cardwell, M.D., Greene, H.W., Hayes, W.K., Hegarty, M.J., Herrmann, H.W., Holycross, A.T., Lannutti, D.I., Mulley, J.F., Sanz, L., Travis, Z.D., Whorley, J.R., Wüster, C.E., Wüster, W., 2019. When one phenotype is not enough: divergent evolutionary trajectories govern venom variation in a widespread

rattlesnake species. Proc. R. Soc. B Biol. Sci. 286. https://doi.org/10.1098/rspb.2018.2735.

Zarzosa, V., Lomonte, B., Zamudio, F., Ponce-López, R., Olvera-Rodríguez, F., Borja, M., Alagón, A., Neri-Castro, E., 2023. Venom of the neotropical rattlesnake, *Crotalus culminatus*: intraspecific variation, neutralization by antivenoms, and immunogenicity in rabbits. Biochimie. https://doi.org/10.1016/j.biochi.2023.10.014.

Zelanis, A., Tashima, A.K., Rocha, M.M.T., Furtado, M.F., Camargo, A.C.M., Ho, P.L., Serrano, S.M.T., 2010. Analysis of the ontogenetic variation in the venom proteome/peptidome of *Bothrops jararaca* reveals different strategies to deal with prey. J. Proteome Res. 9, 2278–2291. https://doi.org/10.1021/pr901027r.